Spring 2024

3D Printed Drone (Body and Controls)

Michael Dick
The University of Akron, mjd171@uakron.edu

Hayden Pinkelman
The University of Akron, htp8@uakron.edu

Tanner Henderson
The University of Akron, tgh18@uakron.edu

Logan Prince
The University of Akron, lep47@uakron.edu

3D Printed Drone (Body and Controls)

Team Members:

Michael Dick - (mjd171@uakron.edu)

Tanner Henderson - (tgh18@uakron.edu)

Hayden Pinkelman - (htp8@uakron.edu)

Logan Prince - (lep47@uakron.edu)

Report for MECE Senior/Honors Design, Spring 2024

Faculty Advisor: Dr. Manigandan Kannan

Faculty/Honors Advisor: Dr. Manigandan Kannan

Faculty/Honors Reader 1: Dr. Yalin Dong

Faculty/Honors Reader 2: Mr. David Peters

Abstract

This project embodies the design and development of a 3D printed drone and encompasses core engineering principles. It begins with aiming for a modular, lightweight, practical, and robust solution. Analysis performed using finite element analysis ensures the structural integrity of the drone. Stable and controlled flight necessitates proficient software and coding knowledge along with controls systems expertise, this project uses an open-source basic flight controller starter code.

Moreover, the project explores the practical application of modern manufacturing techniques, particularly 3D printing technology. This method emphasizes the versatility of manufacturing processes available today and cultivates a deeper understanding of additive manufacturing techniques.

The project extends further into the domain of control systems and coding proficiency. This part is instrumental in ensuring the drone's operational stability, precise control, and optimal flight dynamics. The dynamics of flight control algorithms and systems integration will be essential to a flying drone.

This report serves as a testament to the diligence, rigor, and teamwork applied throughout the project. Furthermore, it also serves as a valuable source of knowledge. It will layout successful methodologies and address potential complications, contributing to a wealth of practical engineering knowledge that future projects can draw upon.

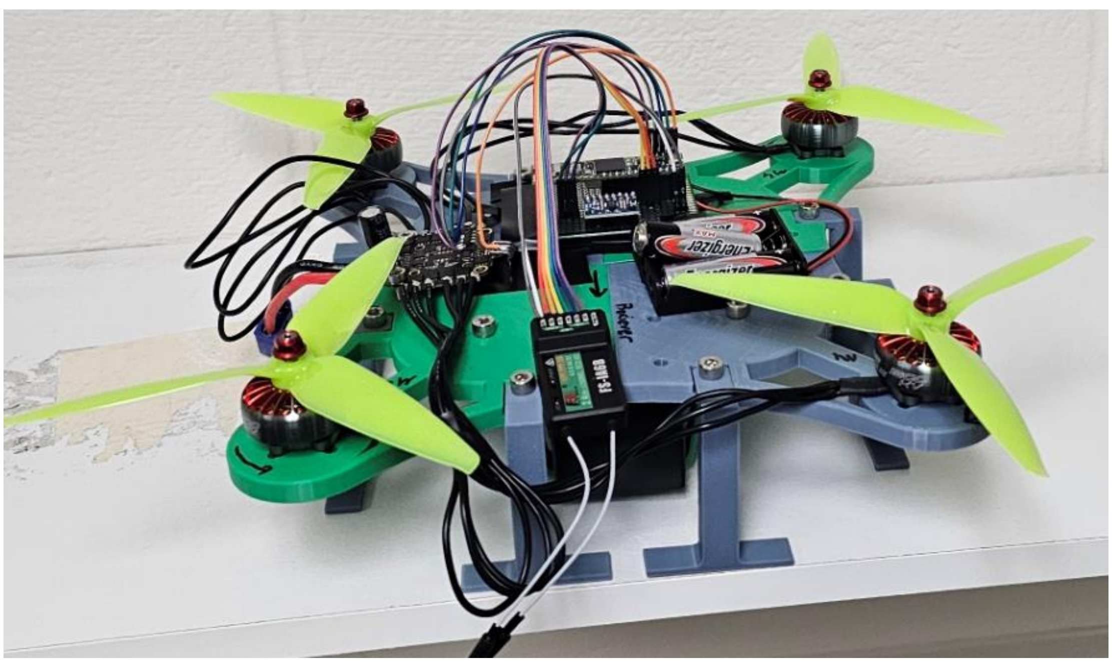

Table of Contents

List of Figures

List of Tables ………………………………………………………………………….. (6)

1. Introduction and Objectives

The primary aim of this project is to design, program, and construct a scalable prototype of a 3D printed drone capable of carrying a load. The idea behind this project is that the drone can be scaled to accommodate whatever payload capacity is chosen by the user for their desired needs, such as package delivery, search and rescue, surveillance, and recreation. The design will be repeatable so that any individual with access to the final report and drawings/files can create a similar drone.

The emphasis on scalability allows for the adaptability and versatility of this drone design. By engineering a system capable of accommodating varying payload sizes, the project acts as a proof of concept for many dynamic and versatile drone applications. This adaptability not only increases the drone's operational usefulness but also widens the avenues of future deployment across a spectrum of scenarios and industries.

All the components the structure team is responsible for will be 3D printed except for the batteries, controls, and receiver. There are numerous advantages of using 3D printing technology such as the ease of access, material versatility, manufacturing simplicity, rapid prototyping, low manufacturing cost, and materials are easy to recycle.

Various materials and filaments will be tested to determine what will provide the optimal ratio of strength to weight while still considering cost. The material must also be rigid, as large deflection in the structure of the drone will cause imbalances that negatively affect the drone's handling and stability.

Despite all the advantages, 3D printing does come with its own downsides. The manufacturing challenges related to 3D printing will be studied, addressed, and solved. Supporting the drone and keeping it stable in flight with a large and potentially unbalanced load will be a heavily focused topic.

For drone enthusiasts, this project presents an exciting avenue for pushing the boundaries of designing and manufacturing an aircraft. The incorporation of 3D printing not only enables the creation of intricate, customized components but also promises greater agility in production. This innovation allows enthusiasts access to a more competitive edge in the rapidly evolving drone industry.

This project holds relevance for a diverse cast of individuals and companies. Drone manufacturers can benefit from the innovative design and manufacturing methodologies employed, potentially opening new avenues for their product lines. Package and food delivery companies could see significant improvements in their operational efficiency and cost-effectiveness through the integration of these advanced drones into their fleets. Furthermore, public health and safety organizations can explore the potential of utilizing these drones for various applications, such as emergency response, surveillance, or environmental monitoring.

Overall, the potential impact of this project extends far beyond the confines of academia, offering tangible benefits to a wide array of industries and sectors. It represents a significant step forward in the integration of cutting-edge technology into real-world applications, with the potential to shape the future of drone-based transportation and services.

2. Field Exploration

To begin the project, we decided to look at current cargo drone offerings to see what design considerations engineers in the drone industry have been making and to become more familiar with the technology used.

2.1 Initial Research

From our initial research, we concluded that it would be impossible to build a drone that can lift 50 lbs with our allotted budget. However, we explored the existing options to gain inspiration for our own cargo drone design.

2.1.1 Current Cargo Drones

Figure 1: DraganFly Heavy Lift Drone

One common cargo drone is the Dragnfly Heavy Lift Drone. It is unique in that it has 6 propellors. This is of large benefit to a payload drone, as it increases total thrust generated. It can lift up to 30 kg. The Draganfly website goes into detail, “The Draganfly Heavy Lift Drone is a versatile, multi-rotor unmanned aerial vehicle (UAV), designed to enhance deliveries and flight times. Compatible with a variety of interchangeable payloads, this heavy-duty drone can carry more and fly longer. The DHL Drone supports automated missions as well as manual flight operations” (Draganfly). The draganfly is a hexacopter drone with a well-engineered design that has set a standard within the UAV industry.

Figure 2: Vulcan UAV D Series (25kg capacity)

An additional drone examined was the Vulcan UAV D Series. It is an 8-prop quadcopter. The additional airfoils allow more thrust to be generated. “With payload capacity up to 15 kg and 25 kg, respectively. These are tough, high resilience aircraft with high payload capacity yet retaining high levels of maneuverability and agility. They are able to handle harsh environments and operational conditions, include a number of configuration options, and can be easily folded for transport. The unusual frame design gives great flexibility in the mounting of payload and sensors and is ideal for applications such as delivery, slung loads, or carrying sensors that need to be separated from the aircraft such as magnetometers” (Vulcan UAV). The Vulcan UAV D series is a quadcopter that was referenced during the initial design and discussion of the drone.

2.1.2 Trends In Current Offerings

A prevalent trend we noticed was the utilization of either quadcopters with counter-rotating motors or drones equipped with more than four arms, a departure from the traditional quadcopter configuration.

This departure is driven by the need for increased payload capacity and stability during flight. By incorporating additional arms, these drones can distribute the weight of the cargo more evenly, enhancing their lifting capabilities.

The counter-rotating motor configuration not only enhances the drone's maneuverability but also contributes to efficient and secure cargo transport. As the demand for aerial logistics continues to rise, these innovative trends signify a shift in the drone industry toward more robust and versatile solutions tailored to meet the evolving needs of consumers.

2.2 Test Drone

The drone we decided to purchase was a DEERC D50 Drone from Amazon to perform some testing and gather baseline data.

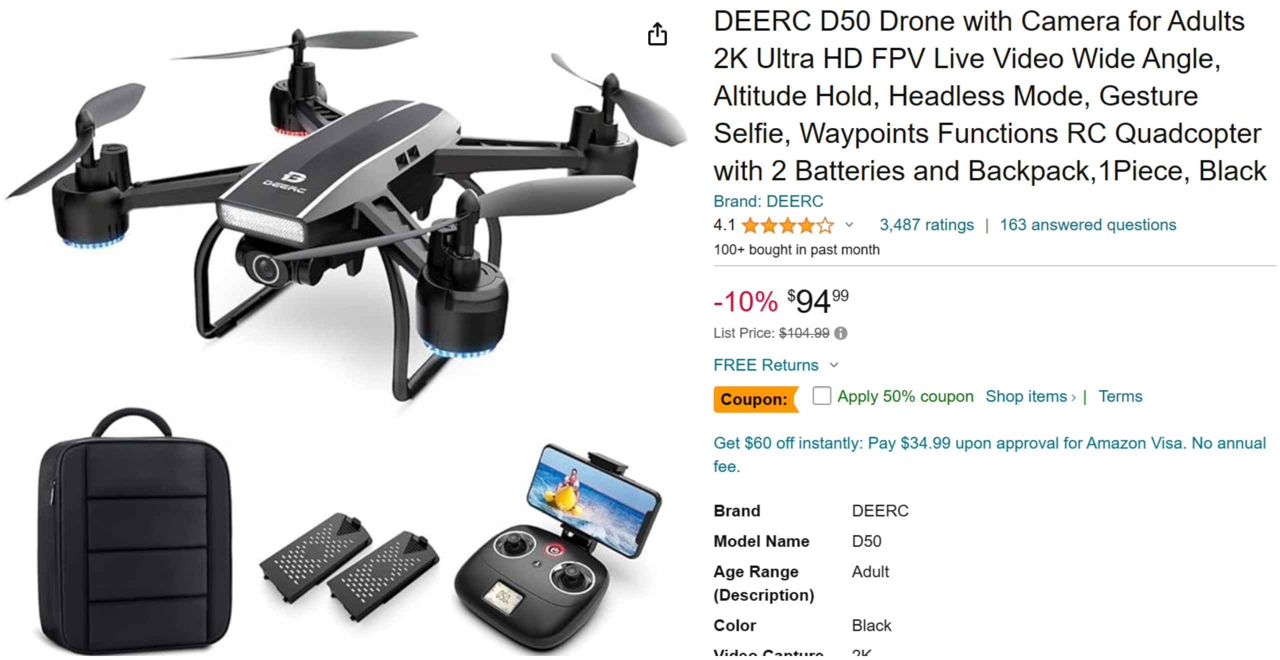

Figure 3: DEERC D50 Drone (Amazon Purchase Page)

2.2.1 Initial Takeaways

The main takeaway of testing the DEERC D50 Drone is that the drone that will be designed in this project will need heavy duty motors capable of generating significant thrust. The test drone weighs 0.405 lbs, yet was only capable of picking up 0.0625 lbs. Furthermore, it was concluded that achieving a low weight and high thrust will likely result in low battery life. When running the test drone at high levels of thrust and motor voltage, the batteries only last around 10-20 minutes until power started significantly decreasing.

2.2.2 Baseline Date

Load (lb)	Analysis
0.25	The drone was unable to move the load at all.
0.125	The drone was able to move the load slightly, however it was extremely unstable and unpredictable. This is roughly the thrust produced.
0.0625	This is the maximum load the drone could lift comfortably. It was able to fly at slow speeds and was controllable.

Table 1: Baseline data (test drone)

3. Initial Design

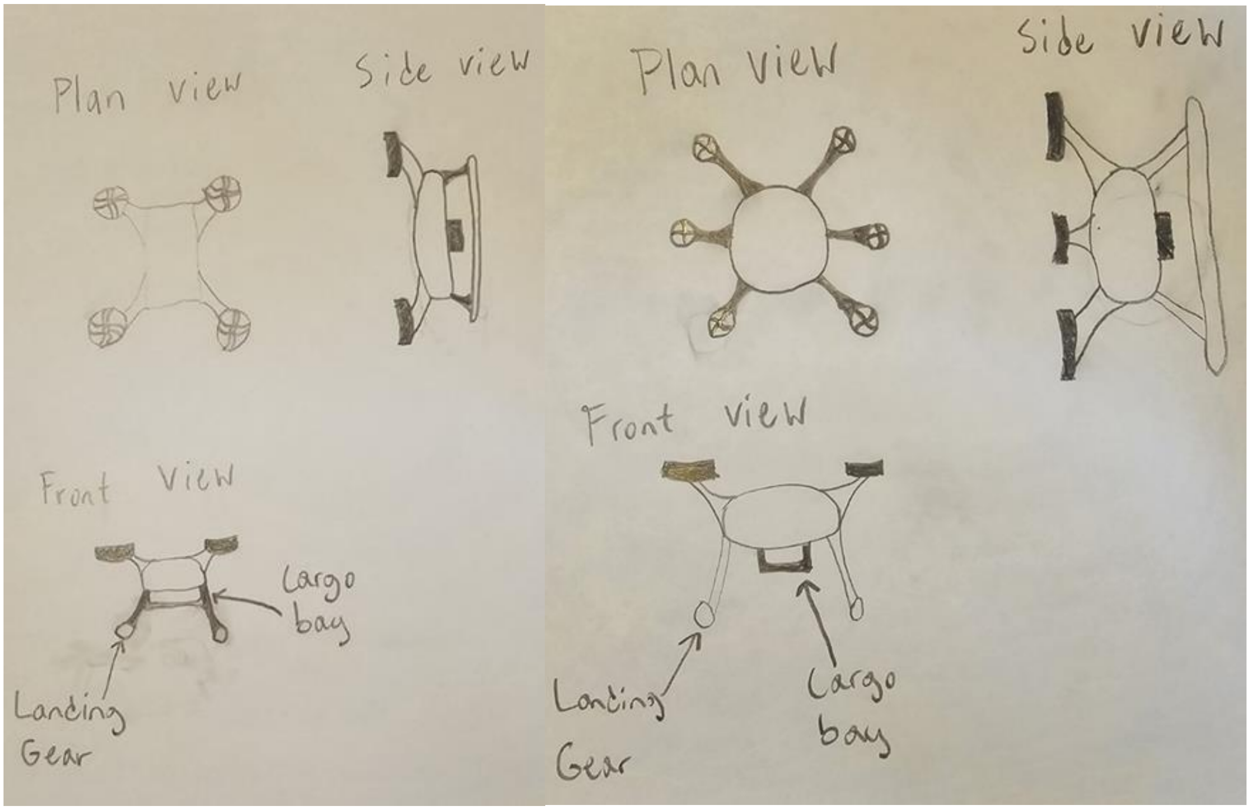

Figure 4: Initial Hexacopter Sketch Idea

Initially, the idea of a hexacopter was thought of, as having two extra arms will provide two additional motors that can generate more thrust. However, as will be explained, this design was not chosen.

3.1 Constraints

There are a variety of constraints that we will use in our design. The first constraint lies in the manufacturing and material selection. We want to create a point of focus around using a widely available, inexpensive, and easy to print material that anyone could print in their home with a regular 3D printer.

Second, there must be multiple holes for cargo bay brackets to bolt onto. The drone can be used for an innumerable amount of cargo, which will be a variety of sizes. Having universal bolt holes on the final design of the drone will allow it to be used for any cargo purpose within specification.

A third constraint that we will follow is modularity of all parts of the drone. This will allow the drone to be easily assembled and disassembled to allow the drone to be easily moved and the parts to be replaced if damage occurs. Furthermore, modular parts make the scaling and manufacturing process better. It allows each piece to be printed by itself if necessary to reach maximum size when scaling.

4. Frame Design

The frame design of this drone went through various redesigns as continuous prototyping resulted in great improvements. The CAD program Inventor was used to design and create drawings of all parts. A factor of safety for the structure of 1.5x to yield stress will be targeted, based upon von Mises stresses. Then, once the drone is built, rigorous testing related to the stability of the drone and the amount of thrust it produces will be done.

4.1 Initial Thoughts & Sketches

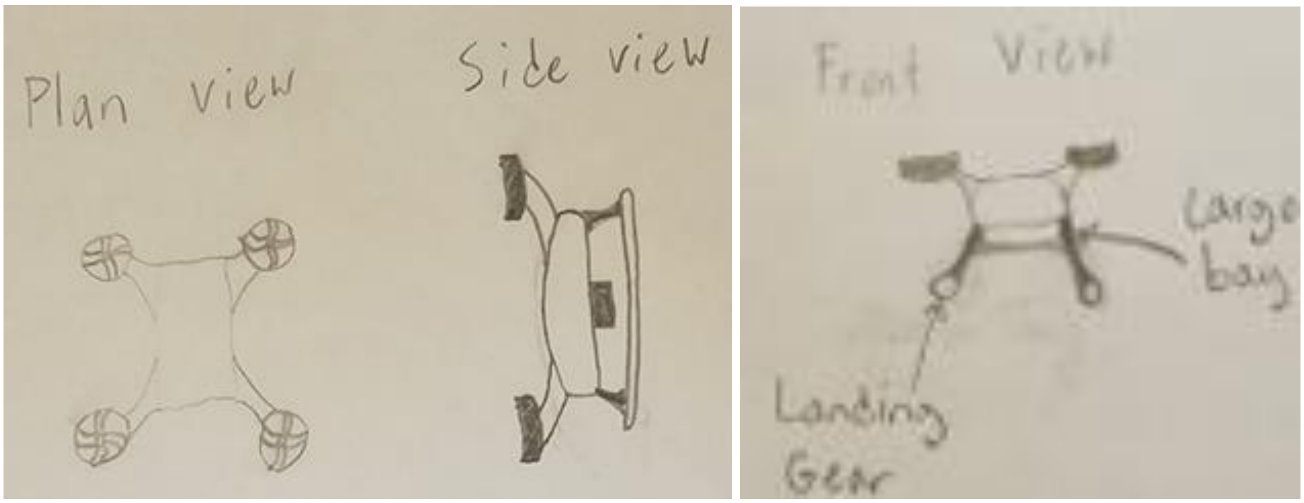

Figure 5: Initial Sketch

Through collaboration with the motor & airfoil group, we decided to design a quad copter for our initial design to reduce weight and unnecessary complexity. Four propellors and 4 motors will supply ample thrust for the purposes of this drone.

4.2 Mk 1.0, First Design

An initial design featured 1 body, 1 cargo bay, 4 legs, and 4 arms. The drone was designed to a large scale, as it was initially planned to use a massive dimension extruder 3d printer. However, the printer was not finished during the time of manufacturing in this project. A Stratasys 3D printer was used to print Mk 1.0 through Mk 2.1. A full prototype of Mk 1.0 was never completed, as the parts were using excessive filament and taking too long to print.

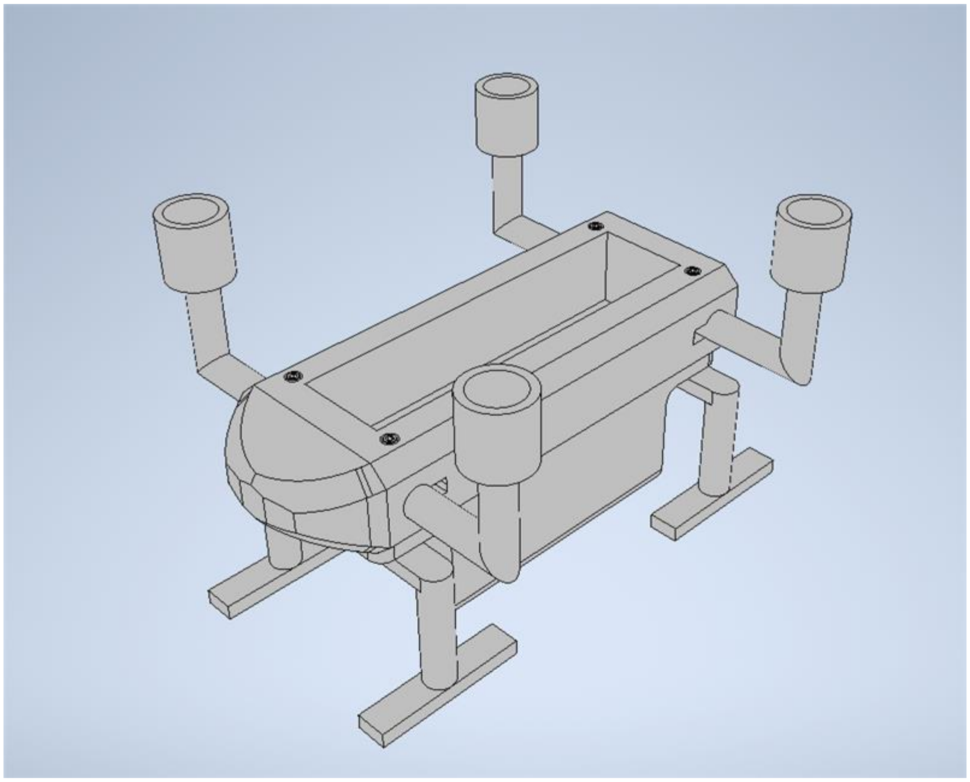

Figure 6: Mk 1.0 Assembly

4.2.1 Body Design

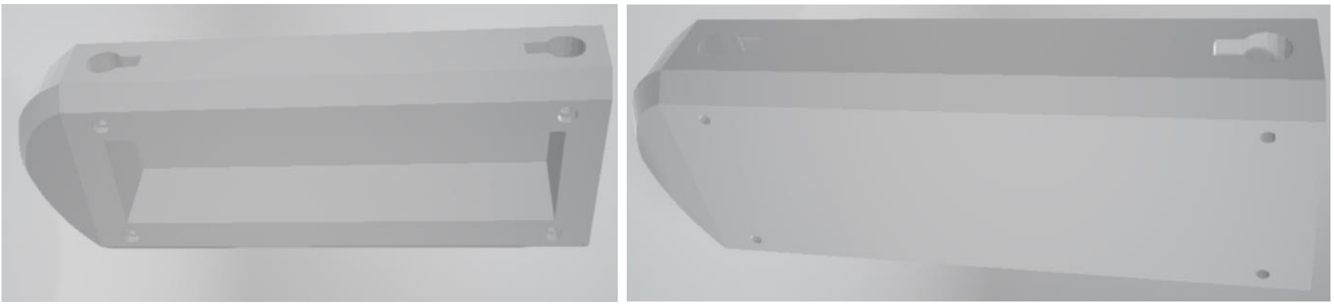

Figure 7: Mk 1.0 Body Design

The body was designed with the idea of both the batteries and the controls being contained within the drone. It also features a keyhole-like design for the arms to go into the body and twist to lock into place. The front of the body has a rounded nose for better aerodynamics.

4.2.2 Cargo Design

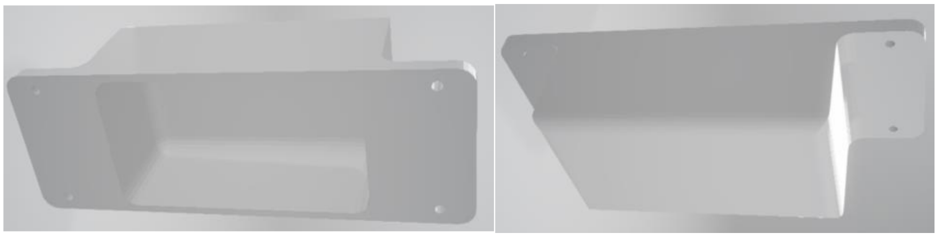

Figure 8: Mk 1.0 Cargo Design

The cargo bay bolts onto the bottom of the body and was designed with plenty of space to carry a load. The cargo bay has flanges on each side to allow space for the landing gear to bolt on.

4.2.3 Arm Design

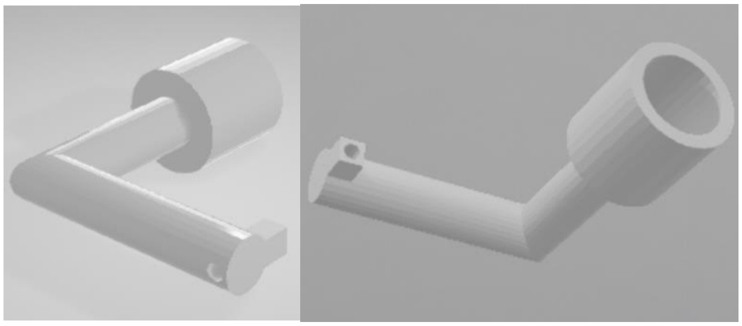

Figure 9: Mk 1.0 Arm Design

The arms are designed with a key-like feature and a hole in the center for a bolt to go through to secure it rigidly in place. The top of the arm has a place holder mounting cylinder for a motor to sit in. This will likely change multiple times throughout the project as we do more testing and change our motors.

4.2.4 Leg Design

Figure 10: Mk 1.0 Leg Design

The leg will bolt to the bottom of the cargo bay. This shape is subject to change after physical testing as well as completion of the finite element analysis simulation.

4.3 Mk 2.0

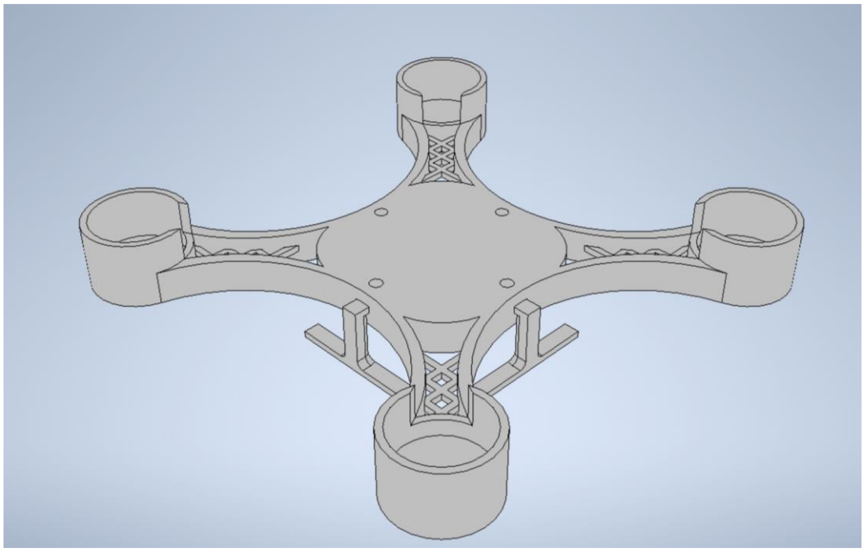

Figure 11: Mk 2.0 Assembly

In this new design, Mk 2.0, we reduced the overall size due to the 3d printer size constraints. Consequently, the weight was significantly reduced. The focus for Mk 2.0 and Mk 2.1 was to get a good single body/arm design, and then make them modular in a future re-design.

4.3.1 Arm Design

Figure 12: Mk 2.0 Arm Design

This arm, which was originally called the “body,” was made with the idea that it could be printed all in one go on an average 3d printer. This would make it easy on the person printing but comes with drawbacks. The first being that the design is not modular. If part of it breaks you must reprint the whole thing over again. The second is that printing it all in one go reduces the size capability of the drone significantly.

4.3.2 Leg Design

Figure 13: Mk 2.0 Leg Design

This was the first iteration of leg design that would eventually end up on our final drone. This leg had some major issues with it on our initial run. The first being that it was too small and due to this it would not print correctly. And consequently because of the small size it was very brittle and would snap easily. The feeling of this is like that of opening a can of soda, which is not brittle if left alone, but put under some stress easily breaks open. Keeping that in mind, when we stress tested our legs, they ultimately ended up snapping very easily.

4.4 Mk 2.1

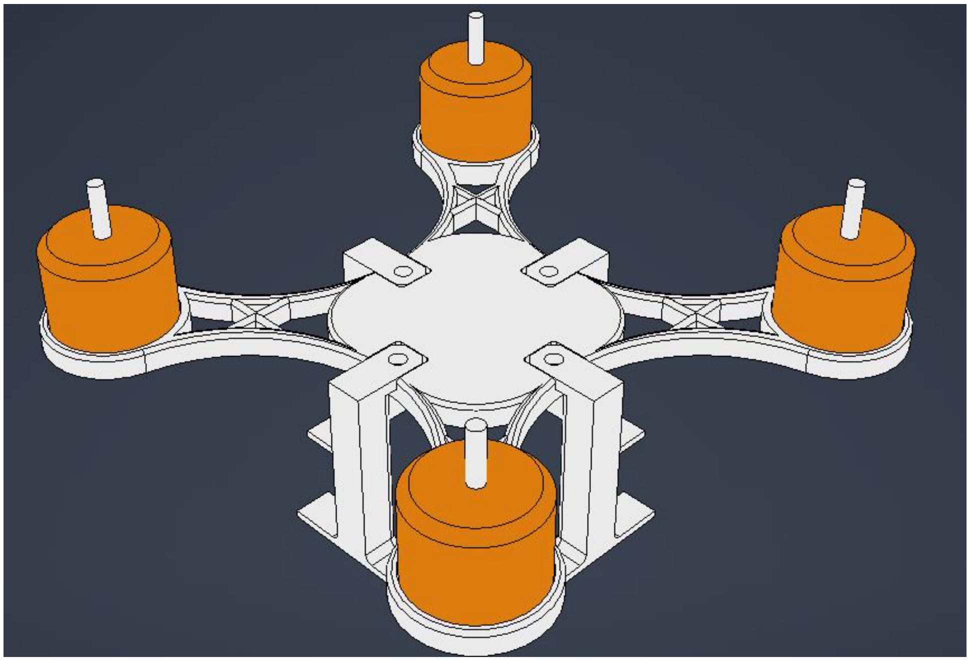

Figure 14: Mk 2.1 Assembly

Taking everything into account from Mk 2.0, we redesigned the drone to be more light weight, while also addressing some concerns from the previous iteration. The weight and the leg brittleness were our main focus of concern for this version, as they were the most critical. This drone served as a foundation for the next redesign.

4.4.1 Arm Design

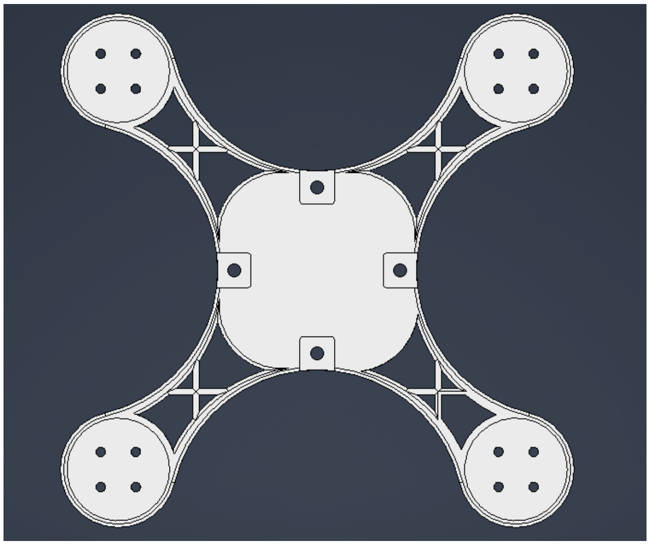

Figure 15: Mk 2.1 Arm Design

In this new body, the thickness was reduced by almost half from Mk 2.0. This was because we found that the original thickness was too robust and that we could reduce it to save weight on the drone. We were also able to cut out some more unnecessary materials, further reducing the weight in the process.

4.4.2 Leg Design

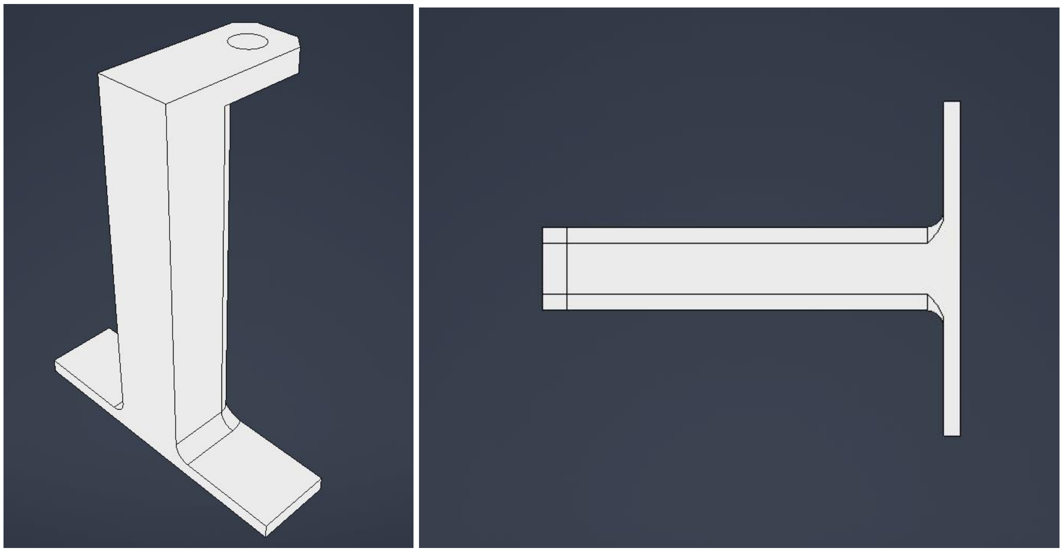

Figure 16: Mk 2.1 Leg Design

This new redesign of the Mk 2.0 Leg is much thicker. However, in practicality we still found this design to break quite often due to material being too small near where the leg bolts into the frame. This would be addressed in our ultimate final design.

4.5 Mk 3.0

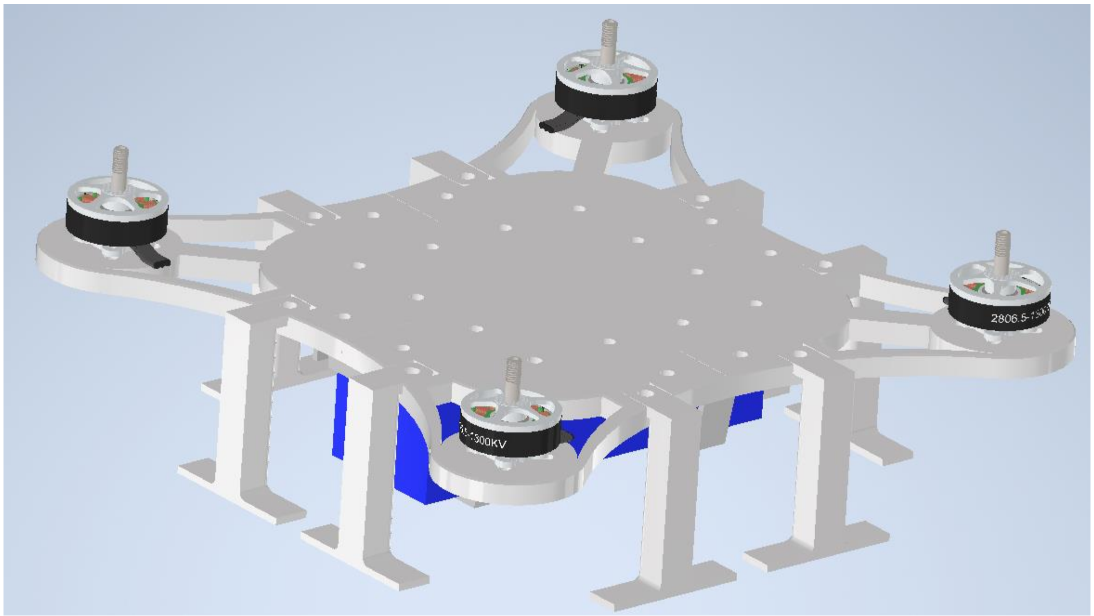

Figure 17: Mk 3.0 Assembly

After careful consideration and testing we decided that we would need a final redesign. In this design we wanted to make the center area of the drone much larger to accommodate for mounting the controls hardware. This design was also made to be more modular so that parts could be replaced more easily. Additionally, this increase in modularity came with a general increase in the size of the drone. While this may create hardships for the 3d printer, this design ultimately ended up superior due to the modularity and the increase in surface area to mount components.

4.5.1 Arm Design

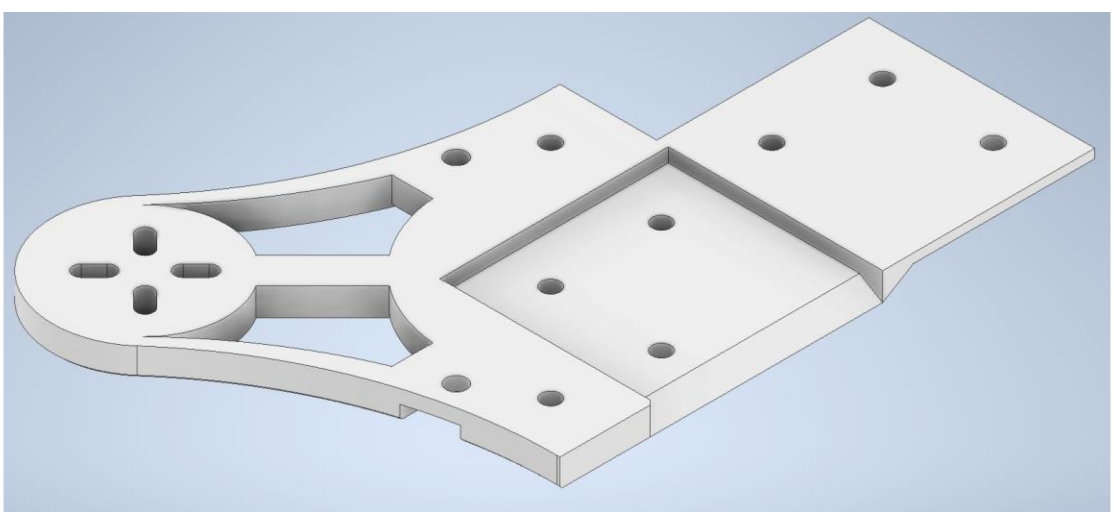

Figure 18: Mk 3.0 Arm Design

This new design of the arm features a “puzzle piece” ability. This means that we are able to print four of the same arm and then put them together like a puzzle. Not only did this make it easy to increase the size of the drone, but it also made the design of the drone faster since we could make one small edit to the arm, and it would affect the whole drone.

4.5.2 Leg Design

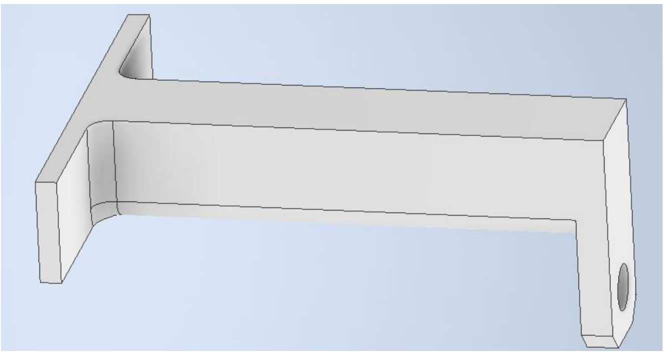

Figure 19: Mk 3.0 Leg Design

This leg is very similar to that of Mk 2.0, the only difference being that it is longer. Furthermore, 8 legs were used for this design to offer additional stability. However, it was discovered this was not necessary. Also, this design moved the mounting of the legs out away from the center of the drone, increasing stability.

4.5.3 Battery Bracket Design

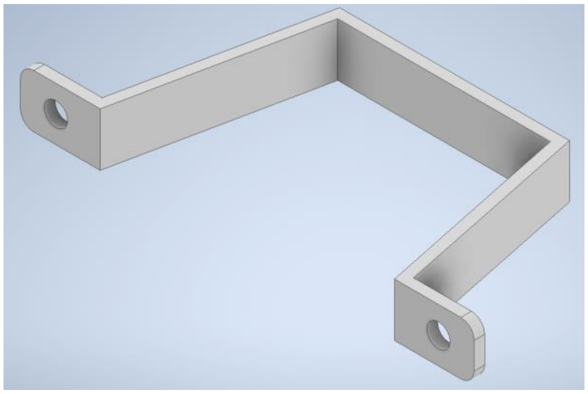

Figure 20: Mk 3.0 Battery Bracket Design

The battery tray was designed and implemented to be bolted through the drone and secures the battery with a snug friction fit. It has a thickness of 0.1 inches.

4.5.4 Brace Design

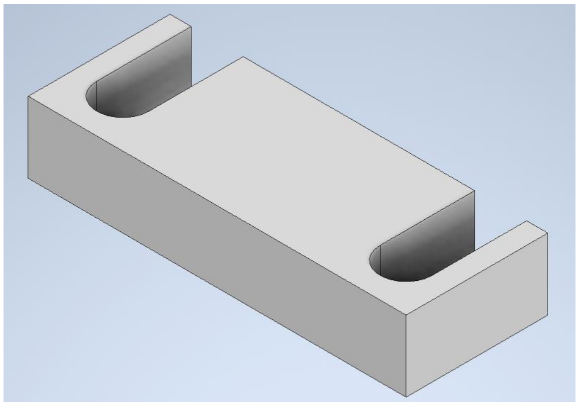

Figure 21: Mk 3.0 Brace Design

The support brace was designed to stiffen the drone frame and reduce flex. The legs were redesigned in Mk 3.1 to solve this stiffness issue without a dedicated support brace.

4.6 Mk 3.1, Final Design

Mk 3.1 represents the final design of the drone and the pinnacle of the engineering experienced in this project. It builds on the success of Mk 3.0, but makes several critical changes to provide an optimal design.

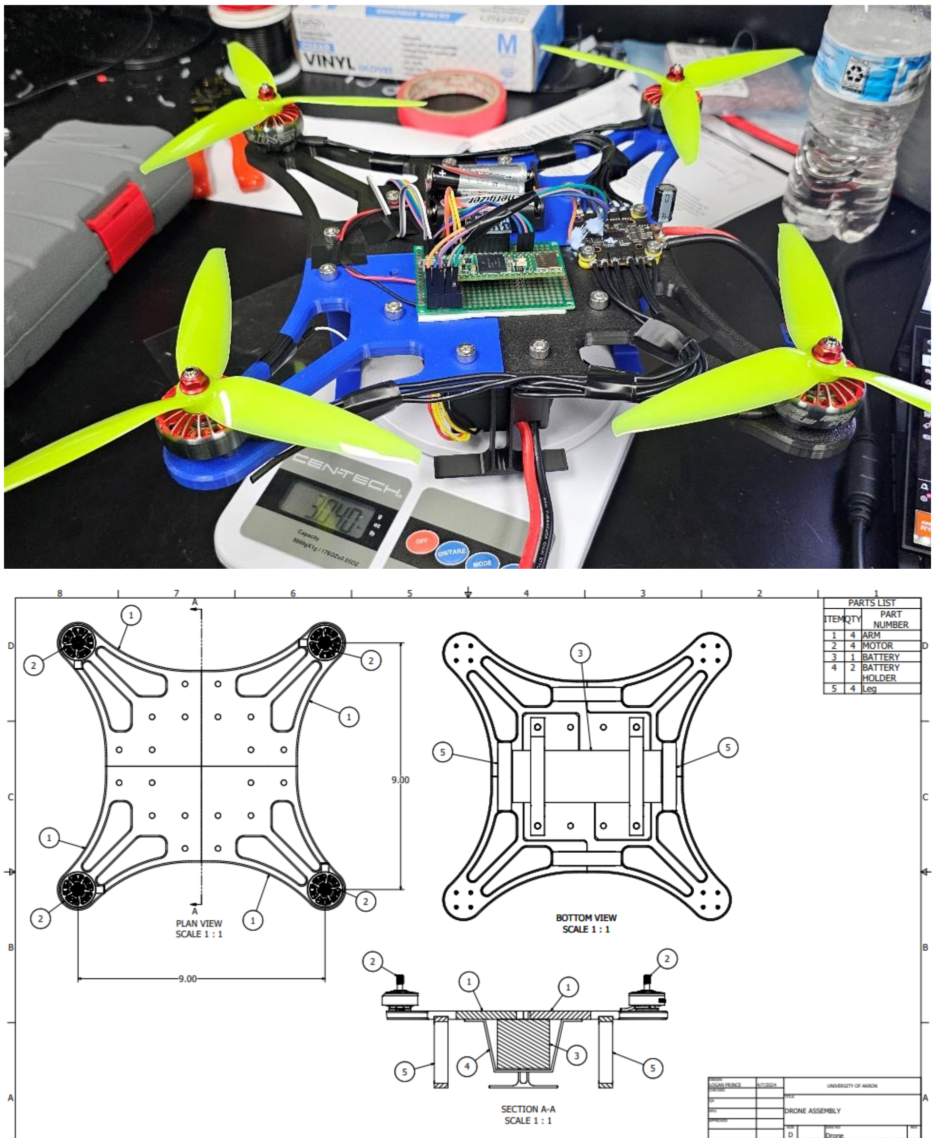

Figure 22: Mk 3.1 Assembly

4.6.1 Arm Design

The motor mounts on the arms were moved out slightly to accommodate for clearance problems experienced on Mk 3.0. Some of the propellors would contact wires if they completed a full rotation on Mk 3.0. This final redesign has solved that problem. Furthermore, now that a final design was reached, various chamfer and edge blends were added to increase strength and functioning of the part. Places where there were stress concentrations had material added to them. Cutouts were added onto the arms for the redesigned legs to slot into.

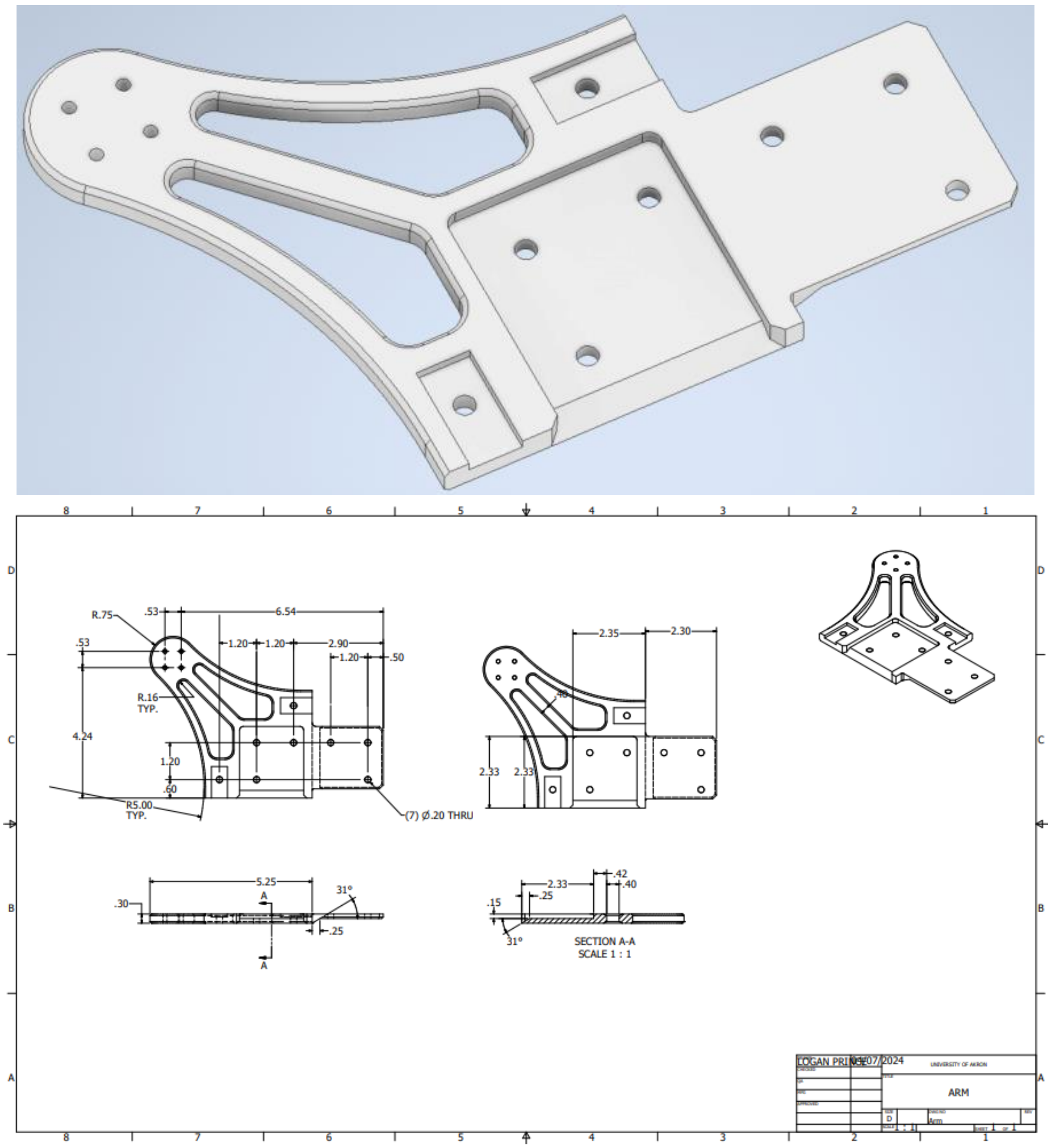

Figure 23: Mk 3.1 Arm Design

4.6.2 Leg Design

After testing Mk 3.0, it was discovered that there is no need for 8 legs for this design. Moreover, the legs have been designed to act as braces. Each leg slots into the arm and then bolts down to provide support. After analyzing the FEA results of Mk 3.0, the legs geometry was redesigned to have a hole in the middle to reduce weight, along with large fillets at various corners. This geometry is ideal, as it focuses material in areas that see stress concentrations in the FEA results.

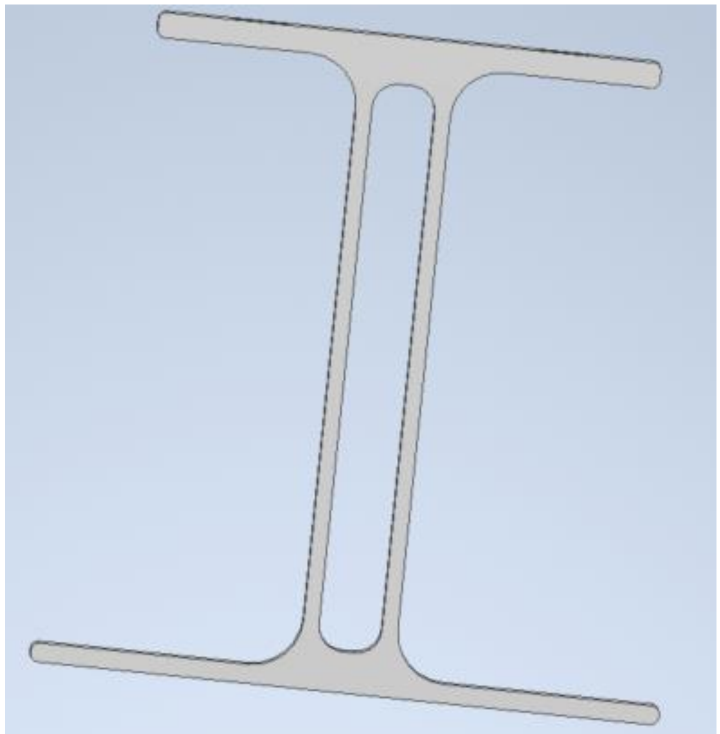

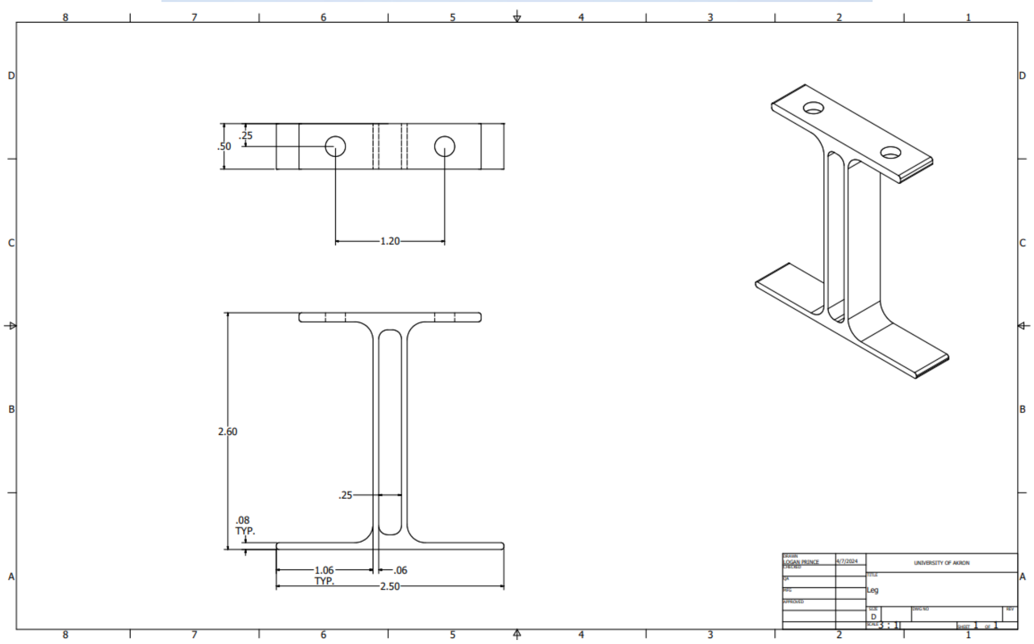

Figure 24: Mk 3.1 Leg Design

4.6.3 Battery Bracket Design

The FEA results for the Mk 3.0 battery bracket saw a factor of safety larger than needed. To reduce weight, the thickness was reduced to 0.075 inches. Various fillets were added to reduce stress concentrations.

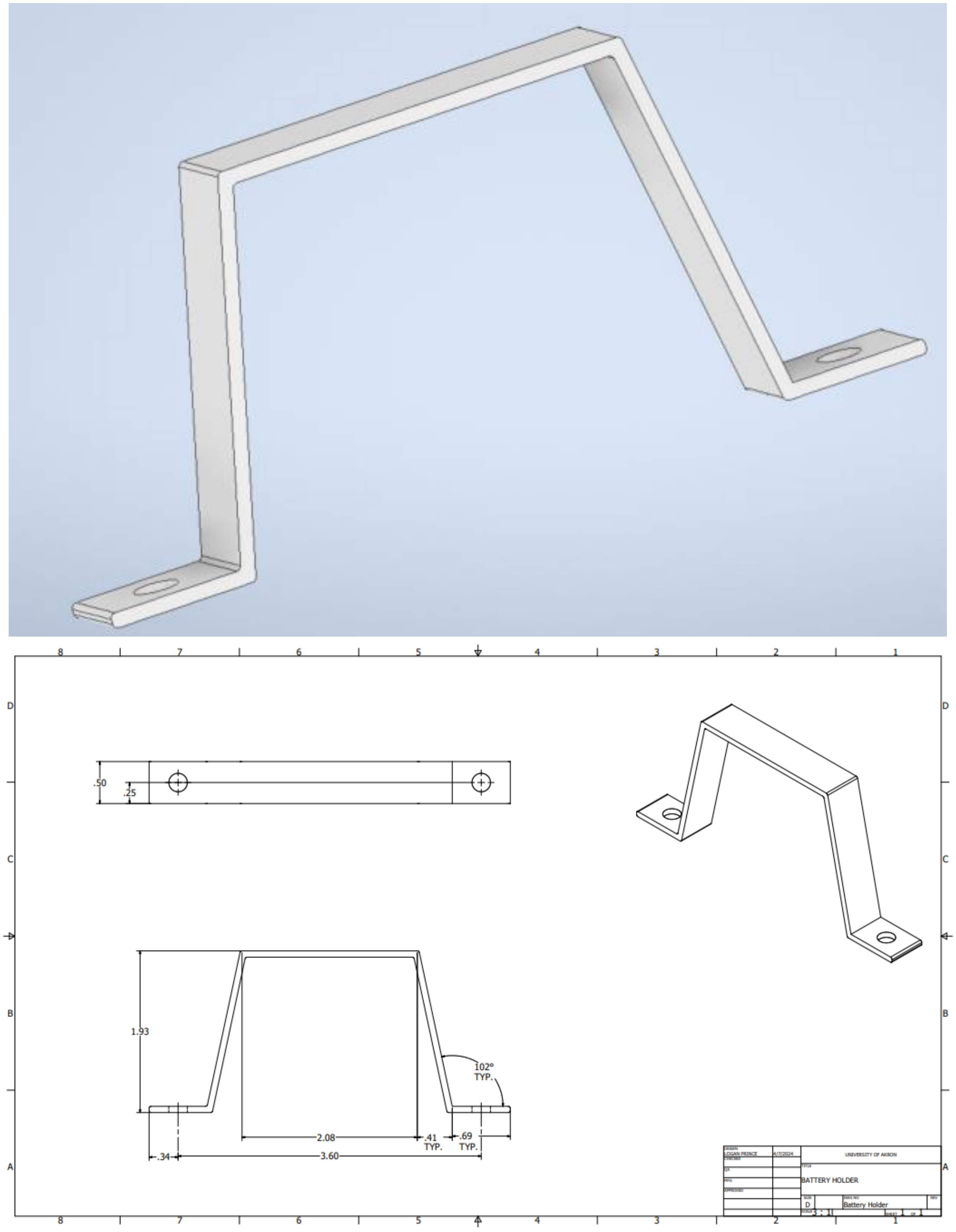

Figure 25: Mk 3.1 Battery Bracket Design

4.7 Final Parts List

All bolts, washers, and nuts were sourced from an Amazon hardware kit. The controls and software related parts were from foreign sources on Amazon. All components designed during the course of the project were 3D printed. The parts list is as follows: (enter parts list)

3D Printed Parts

Name	Quantity	Theoretical Weight (lb)	Actual Weight (lb)	Theoretical Weight (kg)	Actual Weight (kg)	Infill (%)
Arm	4	0.168	0.164	0.076	0.0744	99
Leg	4	0.017	0.016	0.0077	0.0073	99
Battery Holder	2	0.012	0.012	0.00544	0.00544	99
	Total:	0.764	0.744	0.347	0.337	

Outsourced Parts

Name	Quantity	Actual Weight (lb)	Actual Weight (kg)
Gyroscope	1	0.002	0.000907
Micro Controller	1	0.012	0.00544
Transmitter Remote	1	NA (not on drone)	NA (not on drone)
Receiver	1	0.046	0.0209
Battery	1	1.216	0.552
ESC	1	0.032	0.0145
Battery-ESC Wiring	1	0.034	0.0154
Motor	4	0.128	0.0581
Propellor	4	0.018	0.00816
PCB Board	1	0.06	0.0272
Arduino Battery Pack	1	0.172	0.0780
M5 x 12 Bolt	0	0.008	0.00363
M5 x 16 Bolt	8	0.01	0.00454
M5 x 20 Bolt	4	0.01	0.00454
M5 Hex Nut	12	0.002	0.000907
M5 Lock Washer	12	Negligible	Negligible
M4 x 20 Bolt	4	0.004	0.001814
M4 Hex Nut	4	Negligible	Negligible
M4 Lock Washer	4	Negligible	Negligible
M3 x 12 Bolt	16	0.002	0.000907
M3 Hex Nut	16	Negligible	Negligible
M3 Lock Washer	16	Negligible	Negligible
	Total:	2.35	1.066

Table 2: Final Parts List

Once the entire Mk 3.1 drone was complete and put together, it was weighed and a measurement of 3.040 lb was obtained. This is 0.054 lbs less than the measurement of all parts individually. This is due to a buildup of rounding errors caused by the resolution of the Harbor Freight scale used. However, this weight is an acceptable value. While it is not light by any means, the structure is well optimized to lift a heavy load.

A large portion of the weight comes from the battery, which weighs 1.216 lbs. If a large budget were allocated, a more expensive battery with a reduced weight could be purchased. Furthermore, through the design phase several design changes were made to reduce weight. The changes made from Mk 3.0 to Mk 3.1 resulted in reducing the frame weight (arms, legs, braces, battery holder) from 1.06 lbs to 0.744 lbs. This resulted in a significant weight reduction of 29.81%.

5. Controls

While doing background research, it was quickly realized that as Mechanical Engineers, we might be in over our heads for the electrical and controls portion of this project. Having had no prior instruction on the basics of flight controllers or any coding outside of Matlab, and minimal PID controller experience, the best route for the team was to modify previously created code to fit the needs of our project. We decided to use the "dRehmFlight VTOL Flight Controller" documentation created by Nicholas Rehm, since it provides all necessary instructions for creating a basic and easily modified flight controller capable of running our quadcopter. "dRehmFlight is a simple, bare-bones flight controller intended for all types of vertical takeoff and landing (VTOL) vehicles from simple multirotors to more complex transitioning vehicles with a small amount of user modification. This flight controller software and hardware package was developed with people in mind who may not be particularly fluent in object-oriented programming, or software development in general. Other flight controller packages work well for very specific applications, but their extensively developed code bases are not friendly to newcomers looking to hack something together for their new and unique VTOL platform." (Rehm, 2020).

Due to the thoroughness of the dRehmFlight documentation, most of our flight controller hardware and software selections, along with the necessary modifications to implement the code, are pre-determined. These will all be briefly explained in the following sections, and any additional information can be found in the "dRehmFlight VTOL Flight Controller" document referenced at the end of this paper. However, the flight controller is only a small part of the drone's electrical system, and the rest of the components will be more thoroughly explained.

5.1 Software Selection

The software used for the flight controller was downloaded from "dRehmFlight VTOL Flight Controller" and required the use of the *Arduino IDE* platform and "Teensyduino" add-on to upload and run the code. The full code will not be displayed in this report, but it can be accessed through the dRehmFlight GitHub page.

5.2 Hardware Selection

The base necessary control hardware is outlined by the "dRehmFlight VTOL Flight Controller" documentation and consists of several separate components. A Teensy 4.1 microcontroller and a GY-521 MPU6050 IMU were the two main electrical components of the flight controller and were chosen directly from the suggested hardware section of the documentation. Additionally, a double-A battery pack was purchased to power the flight controller, as this was the simplest way to externally power the flight controller without risking damage.

After purchasing the Teensy 4.1 and the MPU-6050 as suggested, we were free to choose the rest of the components on our own, with minimal compatibility restrictions. The FLYSKY FS-i6X transmitter controller with an included FS-iA6B 6-channel PWM receiver was purchased, along with an FS-iA10B 10-channel PWM receiver, which enabled us to add in extra channels and functionality later in the project. This did not end up being used, as we were able to accomplish all of our goals with the 6-channel receiver.

The dRehmFlight documentation was extremely helpful and informative, however it did not take care of everything for us. It did not include any information on motor, ESC (Electronic Speed Controller), or battery selection, obviously crucial to the operation of a quadcopter. Logically, the first step would be to find a motor, however we found that the best place to start is with the ESC, since it has the most restrictive voltage and amperage ratings. After shopping around, the most readily available ESC with the highest amperage rating (45A) while also utilizing the proper Oneshot125 protocol was found and purchased. Next, the four most powerful motors that we could find on Amazon that pulled less than 45 amps each were purchased. After choosing an ESC and motors, the right size battery had to be determined. While researching the use of LiPo batteries on quadcopters, we found that there are two main variables that must be determined. Capacity is measured in mAh, and can be used to find the operating time with the formula T = Cap/1000/A*60, where T is run time in minutes, Cap is capacity, and A is total current draw in amps (Liang, 2023). Using this formula, we were able to estimate a run time of 2.4 minutes for the selected battery, however, it would realistically be much longer since the drone would not be flying at full throttle and the motors draw less current in the real world. The next variable to consider is the C-rating of the battery, which represents the maximum current that can be safely drawn from the battery. This is calculated with the formula M = Cap/1000 * C, where M is maximum current draw in amps, Cap is capacity in mAh, and C is C-rating (Liang, 2023). Using this formula and the battery we had selected; we were able to verify that the C-rating was high enough.

After those main components were selected, the only remaining items that needed to be purchased were small components. The only crucial small component was the adapter to go from ESC to the battery. In addition to that, more generic components were purchased such as wires for connecting components to the Arduino, a perforated solder board to create an elegant flight controller unit, pin headers to connect components to the solder board, and double-A batteries to power the flight controller.

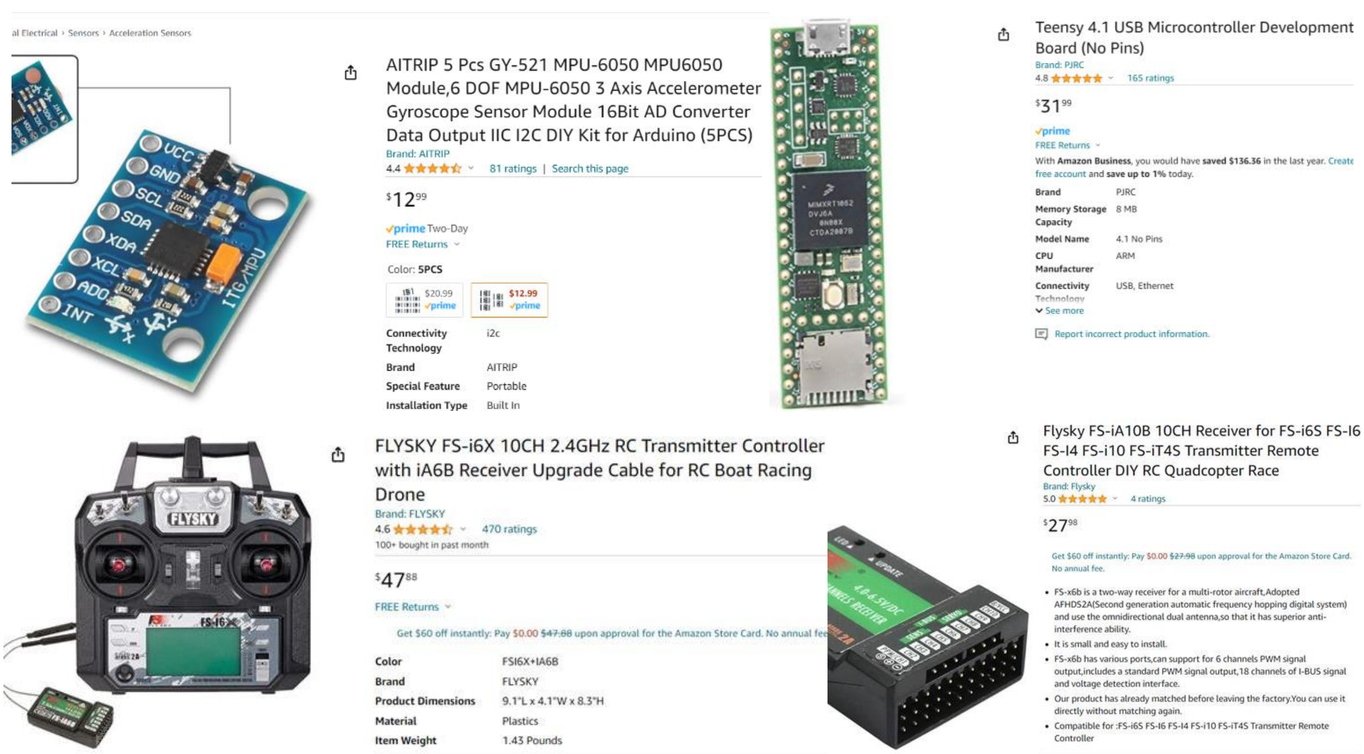

(figure is continued on next page)

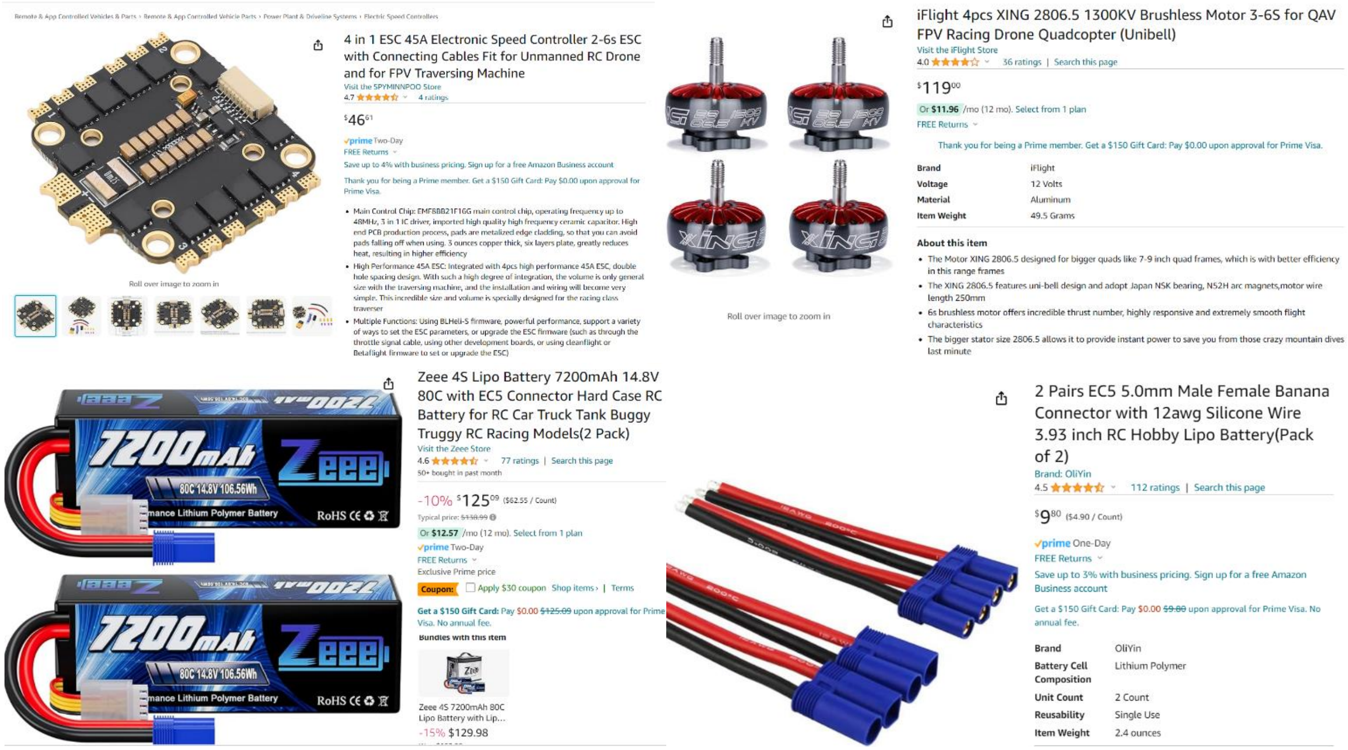

Figure 26: Controls Hardware (Amazon Purchase Page)

5.3 Controls Hardware Assembly

When completing the controls hardware assembly, we decided to solder our main flight controller components onto a perforated solder board. We had intended on using a PCB 3d printer to create a custom PCB board, however that proved to be problematic, and we ended up deciding to use the solder board method. This method allowed us to easily plug and unplug any of our components, while still maintaining a rigid base and promoting good cord management. Also, we had to solder the motor wires, battery connector, and communication wires to the ESC, along with an included capacitor.

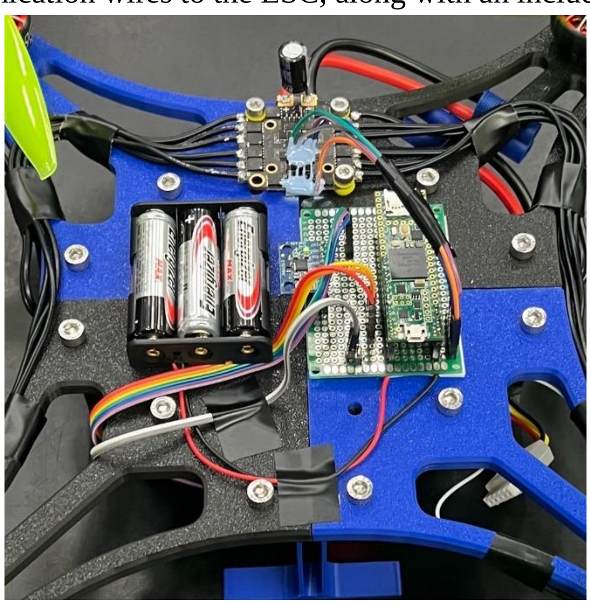
Figure 27: PCB Board and Wiring

5.4 Software Implementation

Once the controls hardware was assembled, the software implementation was extremely simple. The exact steps to get the drone in the air are outlined in the “dRehmFlight VTOL Flight Controller” documentation and consists of several simple tutorials. These include instructions on setting up and verifying radio connection, verifying and calibrating the IMU, control mixing, and selecting and tuning the PID controller. Fortunately, the example PID parameters were good enough to provide us with stable flight, however more intense tuning should be done before the drone is used outside of a testing environment.

Figure 28: Screenshot of Code Use

6. Manufacturing and Material Selection

The criteria for selecting a material for this drone follow: ease of manufacturing, price, strength, and weight. We wanted to create a point of focus around using a widely available, inexpensive, and easy to print material that could be printed with an average 3D printer.

6.1 Initial Manufacturing and Material Options

The initial manufacturing printer planned was going to use pellets in a massive dimension extruder head. The material selection was based on what is available to be used for the general public as well as the MDPH2 – Pellet Head Extruder that was planned on being used for printing the drone:

1. ecoPLAS 3D201
2. LX175 PLA
3. PP Pellets with Carbon Fiber
4. PP Pellets with Glass Fiber

However, the pellet 3D printer that was going to be utilized was a research students' project and was not operational during the time of prototyping for this project. Therefore, alternative 3D printers were considered for manufacturing.

6.2 Final Manufacturing and Material Options

A Stratasys fused deposition modeling (FDM) 3D printer in the University of Akron's 3D printing lab was utilized for designs Mk 1.0 through Mk 2.1. The 3D printer created perfectly manufactured parts. However, lead times spanned several weeks due to a busy engineering lab. A member used the project as an excuse to purchase a Bambu Lab X-1 Carbon Combo FDM 3D printer to significantly shorten lead times. This printer printed all designs Mk 3.0, MK 3.1, and the force testing brackets.

The following materials were selected as possibilities due to their relatively cheap price, availability, and ability to be 3D printed by most 3D printers.'

1. PLA Basic
2. PLA Aero
3. Carbon Fiber Reinforced PA6
4. ABS

(Properties on next page)

Physical Properties		
Subjects	Testing Methods	Data
Density	ISO 1183	1.24 g/cm³
Melt Index	210 °C, 2.16 kg	42.4 ± 3.5 g/10 min
Melting Temperature	DSC, 10 °C/min	160 °C
Glass Transition Temperature	DSC, 10 °C/min	60 °C
Crystallization Temperature	DSC, 10 °C/min	N / A
Vicar Softening Temperature	ISO 306, GB/T 1633	57 °C
Heat Deflection Temperature	ISO 75 1.8 MPa	54 °C
Heat Deflection Temperature	ISO 75 0.45 MPa	57 °C
Saturated Water Absorption Rate	25 °C, 55% RH	0.43%

Mechanical Properties		
Subjects	Testing Methods	Data
Young's Modulus (X-Y)	ISO 527, GB/T 1040	2580 ± 220 MPa
Young's Modulus (Z)	ISO 527, GB/T 1040	2060 ± 170 MPa
Tensile Strength (X-Y)	ISO 527, GB/T 1040	35 ± 4 MPa
Tensile Strength (Z)	ISO 527, GB/T 1040	31 ± 3 MPa
Breaking Elongation Rate (X-Y)	ISO 527, GB/T 1040	12.2 ± 1.8 %
Breaking Elongation Rate (Z)	ISO 527, GB/T 1040	7.5 ± 1.3 %
Bending Modulus (X-Y)	ISO 178, GB/T 9341	2750 ± 160 MPa
Bending Modulus (Z)	ISO 178, GB/T 9341	2370 ± 150 MPa
Bending Strength (X-Y)	ISO 178, GB/T 9341	76 ± 5 MPa
Bending Strength (Z)	ISO 178, GB/T 9341	59 ± 6 MPa
Impact Strength (X-Y)	ISO 179, GB/T 1043	26.6 ± 2.8 kJ/m²; 7.9 ± 1.2 kJ/m² (notched)
Impact Strength (Z)	ISO 179, GB/T 1043	13.8 ± 0.9 kJ/m²

Table 3: PLA Basic Properties

Physical Properties		
Subjects	Testing Methods	Data
Density	ISO 1183	1.21 g/cm³ (filament)
Melt Index	260 °C, 2.16 kg	5.0 ± 0.6 g/10 min
Melting Temperature	DSC, 10 °C/min	154 °C
Glass Transition Temperature	DSC, 10 °C/min	55 °C
Crystallization Temperature	DSC, 10 °C/min	/
Vicar Softening Temperature	ISO 306, GB/T 1633	56 °C
Heat Deflection Temperature	ISO 75 1.8 MPa	50 °C
Heat Deflection Temperature	ISO 75 0.45 MPa	54 °C
Saturated Water Absorption Rate	25 °C, 55% RH	0.48%

Mechanical Properties		
Subjects	Testing Methods	Data
Young's Modulus (X-Y)	ISO 527, GB/T 1040	1670 ± 250 MPa
Young's Modulus (Z)	ISO 527, GB/T 1040	1150 ± 180 MPa
Tensile Strength (X-Y)	ISO 527, GB/T 1040	26 ± 2 MPa
Tensile Strength (Z)	ISO 527, GB/T 1040	14 ± 3 MPa
Breaking Elongation Rate (X-Y)	ISO 527, GB/T 1040	2.2 ± 0.8 %
Breaking Elongation Rate (Z)	ISO 527, GB/T 1040	0.9 ± 0.3 %
Bending Modulus (X-Y)	ISO 178, GB/T 9341	1960 ± 110 MPa
Bending Modulus (Z)	ISO 178, GB/T 9341	1220 ± 80 MPa
Bending Strength (X-Y)	ISO 178, GB/T 9341	42 ± 3 MPa
Bending Strength (Z)	ISO 178, GB/T 9341	15 ± 4 MPa
Impact Strength (X-Y)	ISO 179, GB/T 1043	24.5 ± 1.7 kJ/m²; 7.6 ± 0.9 kJ/m²(notched)
Impact Strength (Z)	ISO 179, GB/T 1043	2.5 ± 0.6 kJ/m²

Table 4: PLA Aero Properties

Physical Properties		
Subjects	Testing Methods	Data
Density	ISO 1183	1.09 g/cm³
Melt Index	280 °C, 2.16 kg	6.8 ± 0.6 g/10 min
Melting Temperature	DSC, 10 °C/min	223 °C
Glass Transition Temperature	DSC, 10 °C/min	68 °C
Crystallization Temperature	DSC, 10 °C/min	185 °C
Vicat Softening Temperature	ISO 306, GB/T 1633	212 °C
Heat Deflection Temperature	ISO 75 1.8 MPa	164 °C
Heat Deflection Temperature	ISO 75 0.45 MPa	186 °C
Saturated Water Absorption Rate	25 °C, 55% RH	2.35%

Mechanical Properties		
Subjects	Testing Methods	Data
Young's Modulus (X-Y)	ISO 527, GB/T 1040	4430 ± 310 MPa
Young's Modulus (Z)	ISO 527, GB/T 1040	2170 ± 230 MPa
Tensile Strength (X-Y)	ISO 527, GB/T 1040	102 ± 7 MPa
Tensile Strength (Z)	ISO 527, GB/T 1040	48 ± 6 MPa
Breaking Elongation Rate (X-Y)	ISO 527, GB/T 1040	5.8 ± 1.6 %
Breaking Elongation Rate (Z)	ISO 527, GB/T 1040	3.7 ± 0.8 %
Bending Modulus (X-Y)	ISO 178, GB/T 9341	5460 ± 280 MPa
Bending Modulus (Z)	ISO 178, GB/T 9341	2240 ± 220 MPa
Bending Strength (X-Y)	ISO 178, GB/T 9341	151 ± 8 MPa
Bending Strength (Z)	ISO 178, GB/T 9341	80 ± 7 MPa
Impact Strength (X-Y)	ISO 179, GB/T 1043	40.3 ± 2.5 kJ/m²; 13.4 ± 1.7 kJ/m² (notched)
Impact Strength (Z)	ISO 179, GB/T 1043	15.5 ± 1.7 kJ/m²

Table 5: Carbon Fiber Reinforced PA6 (Nylon 6) Properties

Physical Properties		
Subjects	Testing Methods	Data
Density	ISO 1183	1.05 g/cm³
Melt Index	260 °C, 2.16 kg	34.2 ± 3.8 g/10 min
Melting Temperature	DSC, 10 °C/min	200 °C
Glass Transition Temperature	DSC, 10 °C/min	N/A
Crystallization Temperature	DSC, 10 °C/min	N/A
Vicar Softening Temperature	ISO 306, GB/T 1633	94 °C
Heat Deflection Temperature	ISO 75 1.8 MPa	84 °C
Heat Deflection Temperature	ISO 75 0.45 MPa	87 °C
Saturated Water Absorption Rate	25 °C, 55% RH	0.65%

Mechanical Properties		
Subjects	Testing Methods	Data
Young's Modulus (X-Y)	ISO 527, GB/T 1040	2200 ± 190 MPa
Young's Modulus (Z)	ISO 527, GB/T 1040	1960 ± 110 MPA
Tensile Strength (X-Y)	ISO 527, GB/T 1040	33 ± 3 MPa
Tensile Strength (Z)	ISO 527, GB/T 1040	28 ± 2 MPa
Breaking Elongation Rate (X-Y)	ISO 527, GB/T 1040	10.5 ± 1.0 %
Breaking Elongation Rate (Z)	ISO 527, GB/T 1040	4.7 ± 0.8 %
Bending Modulus (X-Y)	ISO 178, GB/T 9341	1880 ± 110 MPa
Bending Modulus (Z)	ISO 178, GB/T 9341	1590 ± 100 MPa
Bending Strength (X-Y)	ISO 178, GB/T 9341	62 ± 4 MPa
Bending Strength (Z)	ISO 178, GB/T 9341	39 ± 4 MPa
Impact Strength (X-Y)	ISO 179, GB/T 1043	39.3 ± 3.6 kJ/m²; 21.5 ± 2.2 kJ/m² (notched)
Impact Strength (Z)	ISO 179, GB/T 1043	7.4 ± 1.2 kJ/m²

Table 6: ABS Properties

6.3 Final Material Selected

When first analyzing the material selection, the first property considered was how easy the material is to manufacture. ABS was quickly ruled out due to the failures and warping that can happen when printed without an enclosure or heated bed. A large amount of consumer 3D printers do not have enclosures or heated beds, so printing with ABS is not a suitable option. Next, carbon fiber reinforced PA6 (Nylon), along with all other carbon fiber reinforced materials, were examined. However, carbon fiber is very abrasive, enabling it to wear down standard brass nozzles. Hardened steel nozzles are recommended to use when printing carbon fiber filaments. This makes carbon fiber materials incompatible with the many standard consumer printers, without modification. Therefore, it was ruled out.

Finally, PLA was considered as a material and found to be perfect for the engineering specifications. PLA is very cheap, relatively strong, and is very easy to 3D print. PLA’s low processing temperature allows essentially any FDM 3D printer to print it. There are a large variety of PLA filaments from various manufacturers for different purposes. PLA Basic is the most universal and was chosen as an option. Furthermore, a filament from Bambu Labs called PLA Aero was considered. It is a unique variation of PLA. According to Bambu Labs, “Bambu PLA Aero has almost the same filament density as regular PLA, while the prints density is only 50% to 80%” (Bambu Labs). This is due to PLA Aero foaming at high temperatures during printing. This process causes small holes to form inside of the 3D prints. Foaming PLA materials requires careful calibration of the 3D printer and very precise monitoring and control of the printing temperature. Finally, it is not as durable as regular PLA due to reduced printed density and weight. While PLA Aero is a suitable material, and perhaps even the ideal material for a 3D printed drone, it will not be used because numerous 3D printers will struggle to print with it due to its strict printing requirements.

Figure 29: Bambu Lab Basic Blue PLA

7. Testing

Testing began before the first design was even finished. Various thrust tests were completed on the test drone purchased to determine what loads the drone can lift. The tests also provided baseline data to show the relationship between thrust and payload capacity.

7.1 Test Drone Flight Test Setup

Figure 30: Initial Test Setup – (The left image shows flight testing, the image to the right shows thrust testing)

Figure 31: DEERC D50 Test Drone

7.2 Test Drone Initial Findings

Load (lb)	Analysis
0.25	The drone was unable to move the load at all.
0.125	The drone was able to move the load slightly, however it was extremely unstable and unpredictable.
0.0625	This is the maximum load the drone could lift comfortably. It was able to fly at slow speeds and was controllable. This establishes that drones can have stable with a payload with a value up to half of the drone's total thrust.

Table 1: Test Drone Baseline Data

7.3 PLA Material Analysis

Bambu Labs supplies a significant amount of material data to aid in analysis and testing. However, they never provide any data on yield strength. While it is likely that a complete failure of a PLA part would be from an ultimate failure, the yield strength is important to consider for a factor of safety and to prevent extremely large deformations that can have negative effects on the flight dynamics of the drone. A recent study done on PLA material properties states, "Its optimum mechanical property is 32.938 MPa for ultimate tensile strength, 807.489 MPa for elastic modulus and 26.082 MPa for yield strength" (Sounders, 2019). While this data was taken from a PLA sourced from a different manufacturer and was printed on a different 3D printer than what will be used, it provides a good benchmark for designing. This study was done using 80% infill. 99% infill was used to ensure all finite element analysis calculations are as close to real life as possible.

An additional property not given by Bambu Lab was shear modulus. Ansys finite element analysis needs this value to model an orthotropic material, like 3D printed PLA. The Bambu Labs PLA technical data sheet does not supply the shear modulus for each axis. The relationship between shear modulus and the supplied Young's Modulus for isotropic materials was used below. While this relationship is for isotropic materials, it will provide an estimate of the value. Bambu Lab does not give any Poisson ratio data either. Both of the equations shown below were used to calculate the missing material data.

E is the Young's Modulus. G is the shear modulus. "v" is the Poisson ratio.

$$G = \frac{E}{2*(1+v)} \qquad v = \frac{E}{2*G} - 1$$

Bambu Lab PLA Material Properties		
Type	Metric Value	Imperial Value
Young's Modulus X	2580 MPa	374197.364 psi
Young's Modulus Y	2580 MPa	374197.364 psi
Young's Modulus, Z	2060 MPa	298777.74 psi
Poisson's Ratio XY	0.3	0.3
Poisson's Ratio YZ	0.3	0.3
Poisson's Ratio XZ	0.3	0.3
Shear Modulus XY	992.31 MPa	143922.398 psi
Shear Modulus YZ	992.31 MPa	143922.398 psi
Shear Modulus XZ	792.31 MPa	114914.85 psi
Tensile Strength X	35 MPa	5076.32 psi
Tensile Strength Y	35 MPa	5076.32 psi
Tensile Strength Z	31 MPa	4496.17 psi
Density	1.24 g/cm^3	0.04479 lb/in^3
Yield Stength (estimated)	26.082 MPa	3782.87 psi

Table 7: Bambu Lab PLA Material Properties

7.4 Mk 1.0 Testing

No physical or finite element analysis was completed on Mk 1.0. This first design was an initial proof of concept to begin the design process. It was the first step in the design process journey.

7.5 Mk 2.0 Testing

ANSYS Finite Element Analysis was used to analyze the stress and deformation values the drone parts will see during operating conditions. All mesh sizes were 0.05 inch, along with adaptive mesh refinement with 10 max loops and refinement depth of 2.

To use finite element analysis to analyze Mk 2.0 arms, each arm was divided into single part so that a single arm can be simulated. This provides more accurate analysis than simulation of the entire assembly. It was simulated similarly to a cantilever beam, where the force is at the end of each arm on the top and bottom face of the motor mount area, and the fixed supports are at the opposite end on the side faces. A maximum stress of 3139 psi was calculated from a force of 4.50 lbf. With an estimated yield strength of 3782.87 psi, this produces a factor of safety of 1.205.

This force was calculated by dividing the full weight of the drone and cargo by 4, to account for all four arms. A theoretical total weight of 6 lbs is used. Then, an acceleration of 3 times gravity was multiplied to it.

$$F = m * a = mass\ times\ acceleration$$

$$4.50\ lbf = 1.50\ lb * 32.2 \frac{ft}{s^2} * 3 * \frac{lbf * s^2}{32.2\ lb * ft}$$

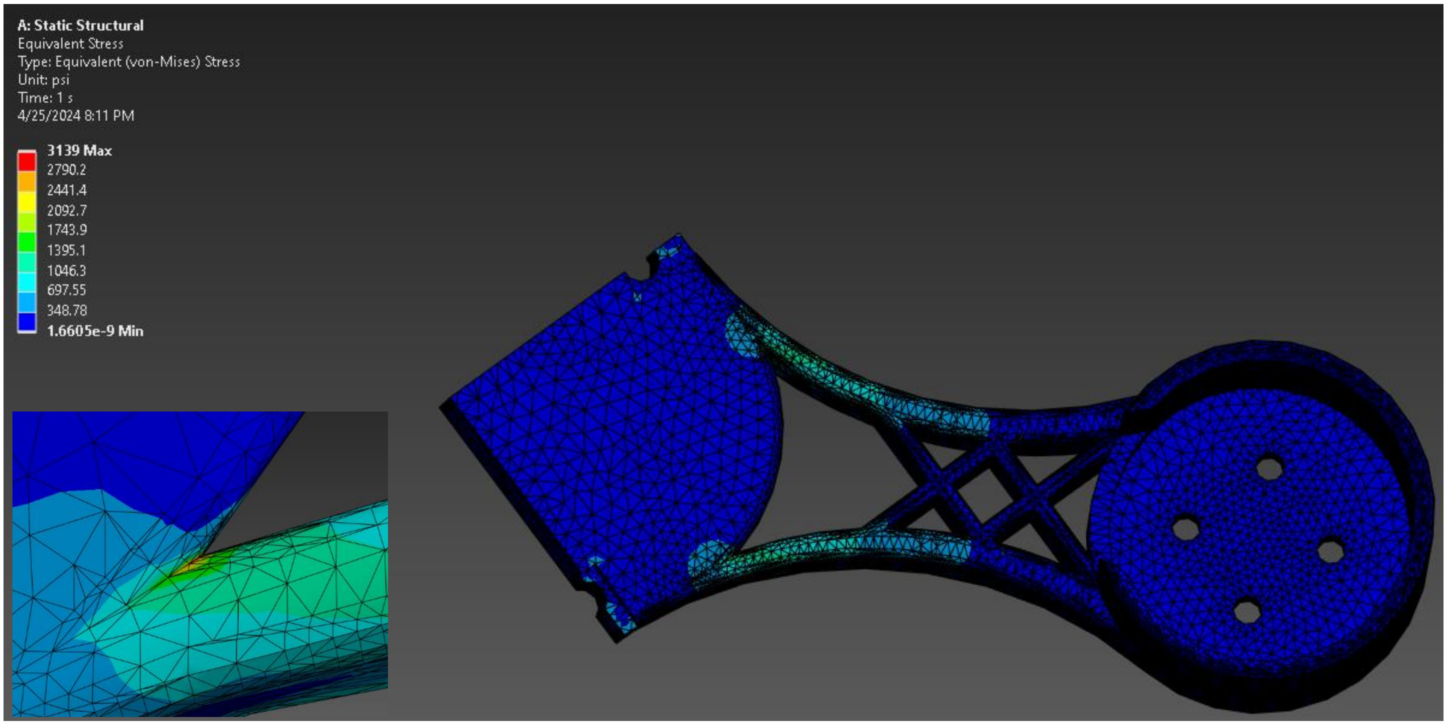

Figure 32: (Mk 2.0 FEA) – Arm

Each leg was simulated for two failure modes: one where an upwards force is experienced on the bottom of the leg's face, and one where the leg experiences a force from the side. Both failures would require a collision to occur during flight of the drone, so the values of the forces are estimates.

When the drone is impacted on the bottom face of the leg by an upward force of 6.0 lbf, a maximum stress of 2553.8 psi was calculated. With an estimated yield strength of 3782.87 psi, this produces a factor of safety of 1.48.

This force was calculated using the same method as the arm, except an acceleration of 4 times gravity was used due to the likelihood of an unplanned descent event causing a large impact to the legs. Then, an acceleration of 4 times gravity was multiplied to it.

$$6.0\ lbf = 1.50\ lb * \ 32.2\frac{ft}{s^2} * \ 4 * \frac{lbf * s^2}{32.2\ lb * ft}$$

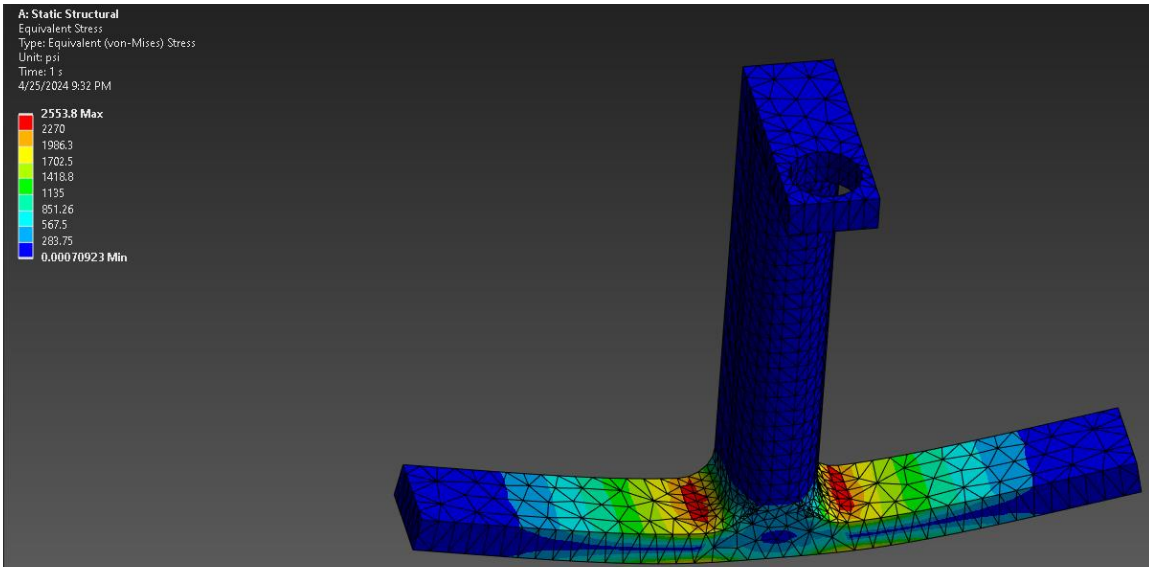

Figure 33: (Mk 2.0 FEA) – Leg, Upward Force

When the leg is impacted on the side face of the bottom part of the leg by a side force of 4 lbf, a maximum stress of 3192.8 psi was calculated. With an estimated yield strength of 3782.87 psi, this produces a factor of safety of 1.18.

This force was calculated using the same method as the arm, except an acceleration of 2.67 times gravity was used since it is unlikely the drone will be impacted in this manner. It is likely a side impact of this nature would also hit the propellors, which would fail before the legs.

$$4.0\ lbf = 1.50\ lb * 32.2\frac{ft}{s^2} * 2.67 * \frac{lbf * s^2}{32.2\ lb * ft}$$

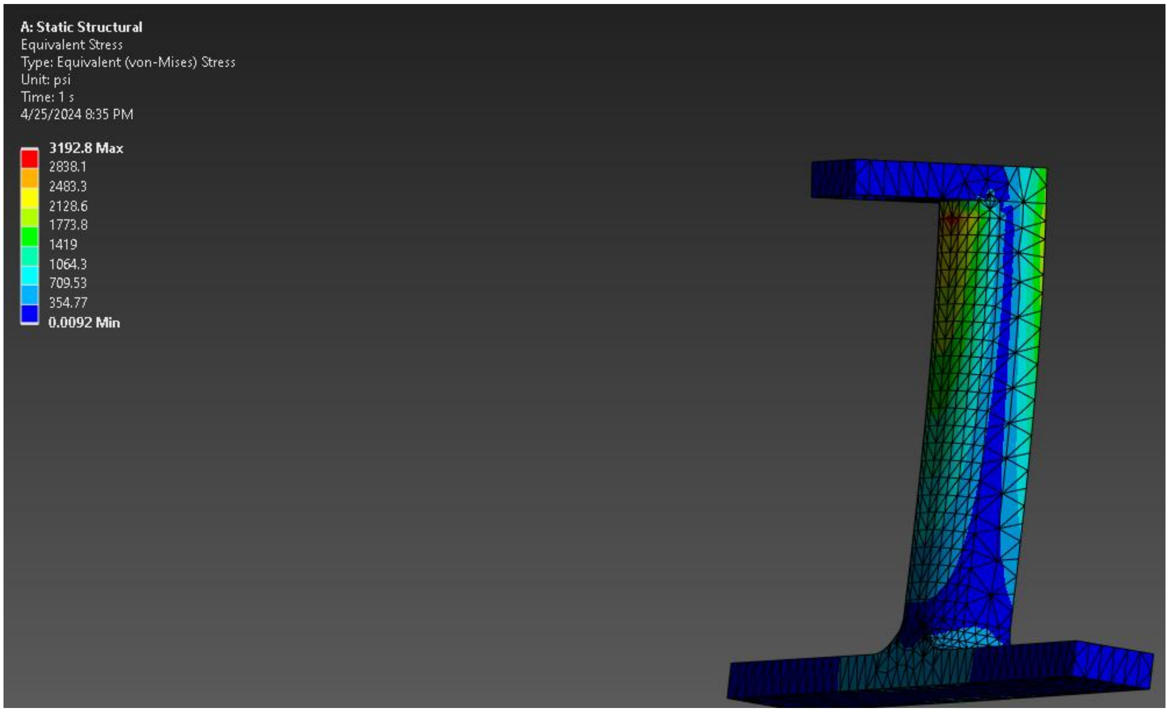

Figure 34: (Mk 2.0 FEA) – Leg, Side Force

7.6 Mk 2.1 Testing

All mesh sizes were 0.05 inch, along with adaptive mesh refinement with 10 max loops and refinement depth of 2. All parts in Mk 2.1 were simulated using the same supports and force values and locations in Mk 2.0

For each arm, a maximum stress of 7603.9 psi was calculated from a force of 4.50 lbf. With an estimated yield strength of 3782.87 psi, this produces a factor of safety of 0.5. This failure encouraged a further redesign of the entire drone. The maximum stress is a stress concentration seen at the corners of the geometry that bridge out to the motor mounts. Future designs will fix this issue.

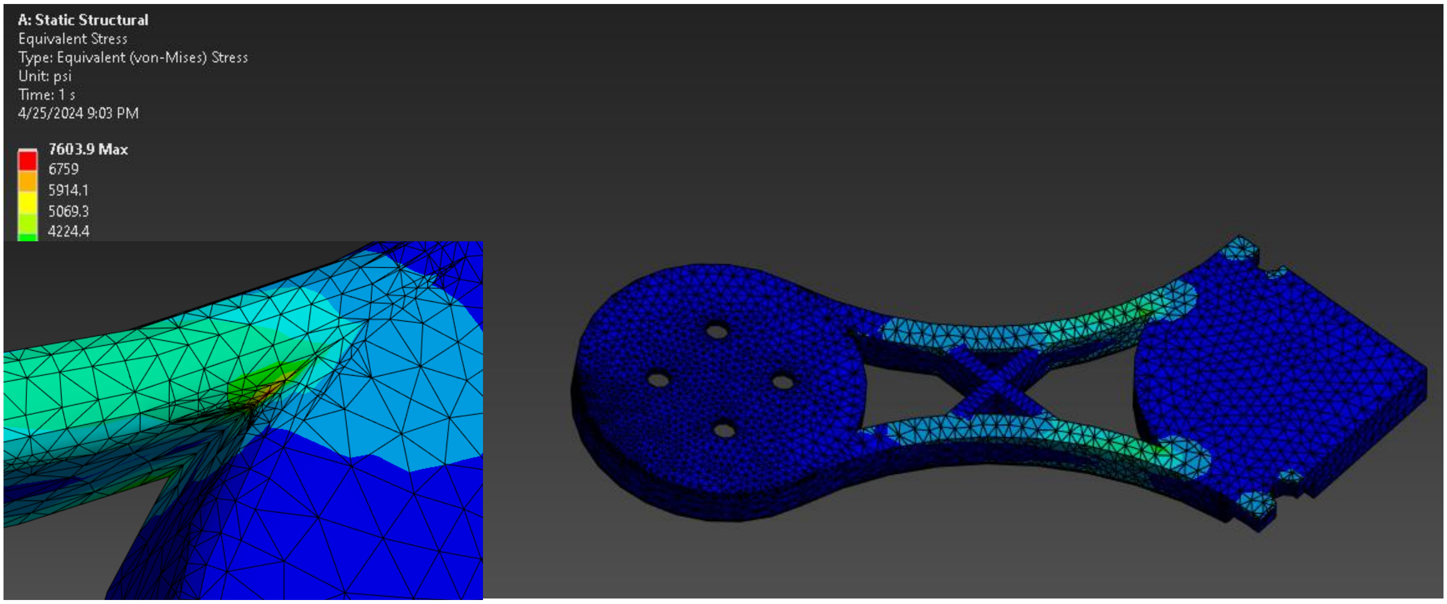

Figure 35: (Mk 2.1 FEA) – Arm

When the drone is impacted on the bottom face of the leg by an upward force of 6.0 lbf, a maximum stress of 1948.2 psi was calculated. With an estimated yield strength of 3782.87 psi, this produces a factor of safety of 1.94

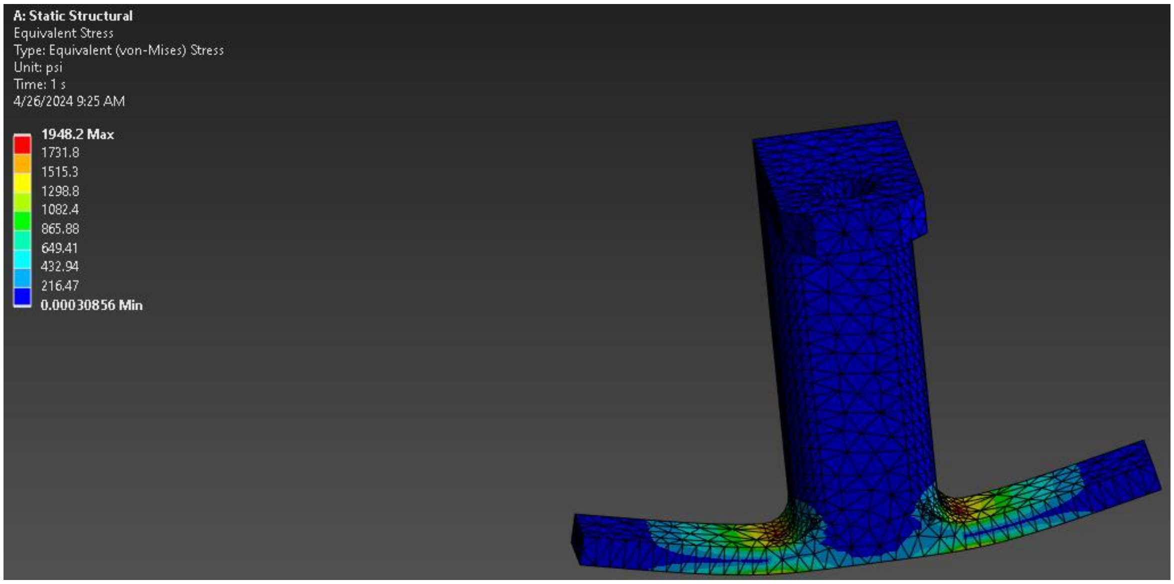

Figure 36: (Mk 2.1 FEA) – Leg, Upward Force

When the leg is impacted on the side face of the bottom part of the leg by a side force of 4 lbf, a maximum stress of 1350.4 psi was calculated. With an estimated yield strength of 3782.87 psi, this produces a factor of safety of 2.801.

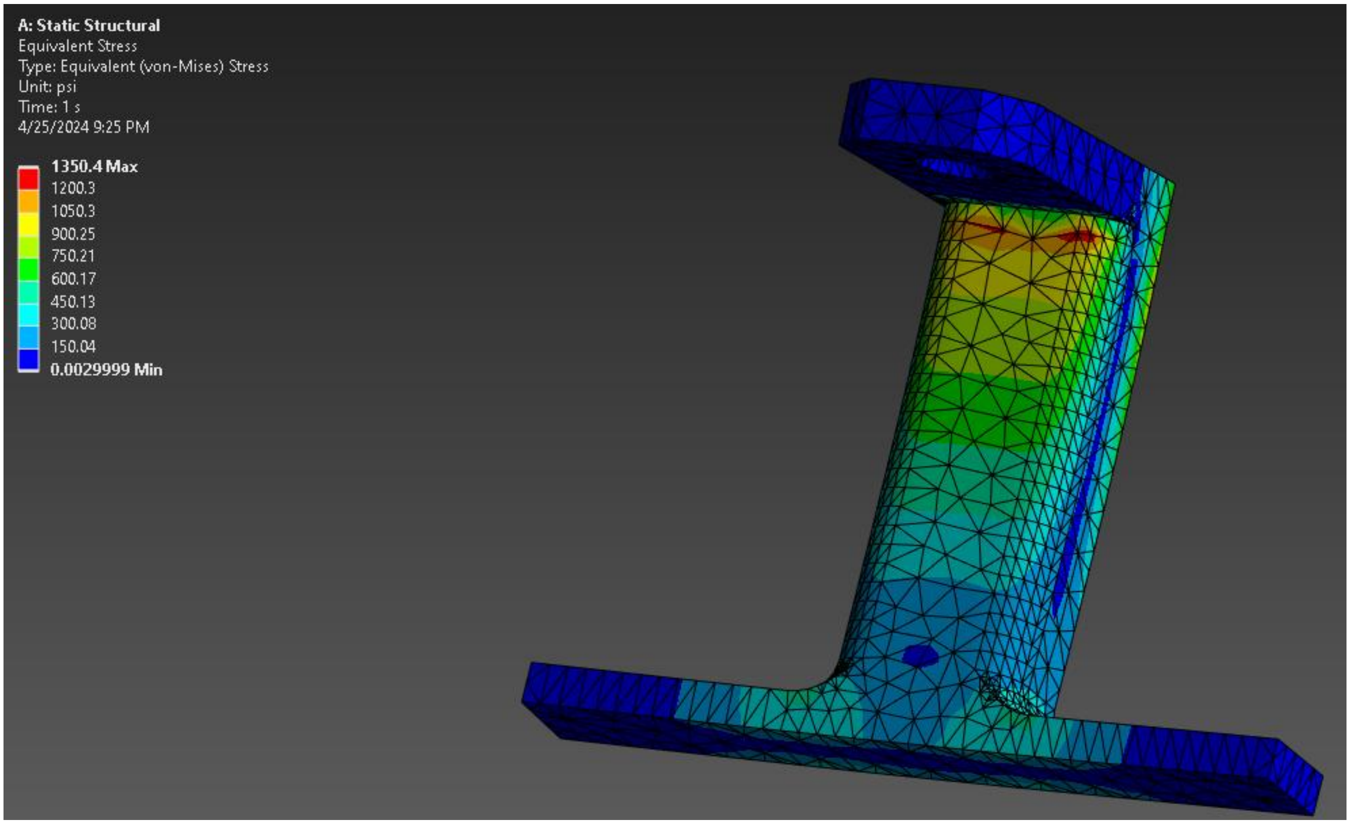

Figure 37: (Mk 2.1 FEA) – Leg, Side Force

7.7 Mk 3.0 Testing

All mesh sizes were 0.05 inch, along with adaptive mesh refinement with 10 max loops and refinement depth of 2. The arms and legs were simulated using the same conditions as in Mk 2.0 and Mk 2.1.

For each arm, a maximum stress of 1424.8 psi was calculated from a force of 4.7145 lbf. With an estimated yield strength of 3782.87 psi, this produces a factor of safety of 2.66. At this part in the design phase, enough information was known about the parts of the drone to start using calculating weight values. For this design, hardware, and a cargo of 3 lbs, a total weight of 6.286 lbs was calculated.

$$F = m * a = mass\ times\ acceleration$$

$$4.7145\ lbf = 1.5715\ lb * 32.2\frac{ft}{s^2} * 3 * \frac{lbf * s^2}{32.2\ lb * ft}$$

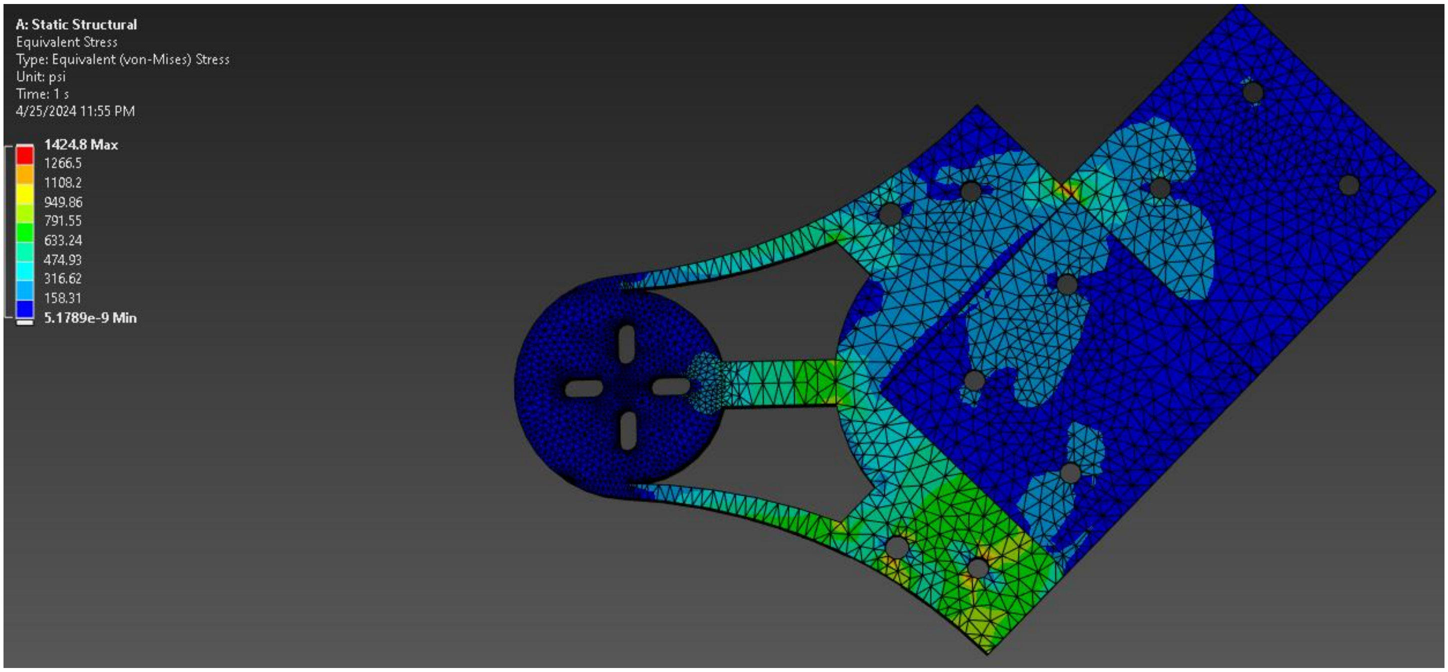

Figure 38: (Mk 3.0 FEA) – Arm

When the drone is impacted on the bottom face of the leg by an upward force of 6.286 lbf, a maximum stress of 935.35 psi was calculated. With an estimated yield strength of 3782.87 psi, this produces a factor of safety of 4.04.

$$6.286\ lbf = 1.5715\ lb * \ 32.2\frac{ft}{s^2} * \ 4 * \frac{lbf * s^2}{32.2\ lb * ft}$$

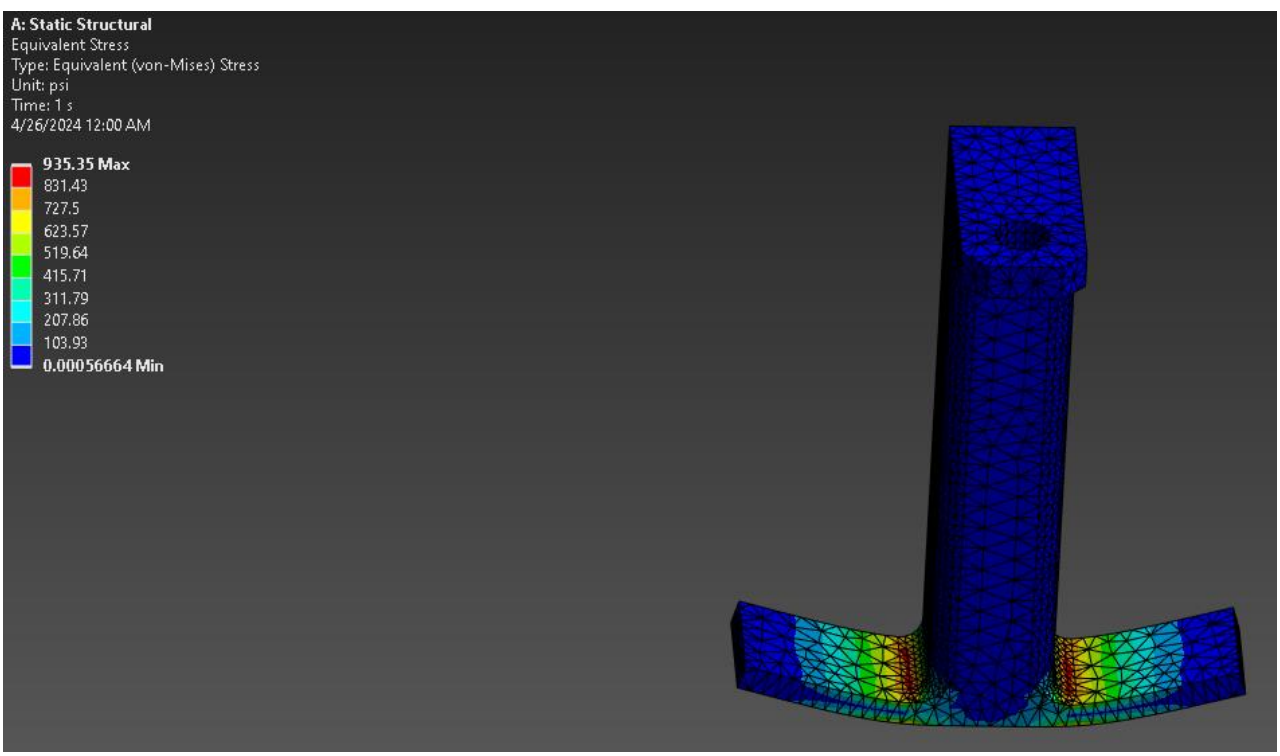

Figure 39: (Mk 3.0 FEA) - Leg, Upward Force

When the leg is impacted on the side face of the bottom part of the leg by a side force of 4.20 lbf, a maximum stress of 650.78 psi was calculated. With an estimated yield strength of 3782.87 psi, this produces a factor of safety of 5.81.

$$4.20\ lbf = 1.5715\ lb * \ 32.2\frac{ft}{s^2} * \ 2.67 * \frac{lbf * s^2}{32.2\ lb * ft}$$

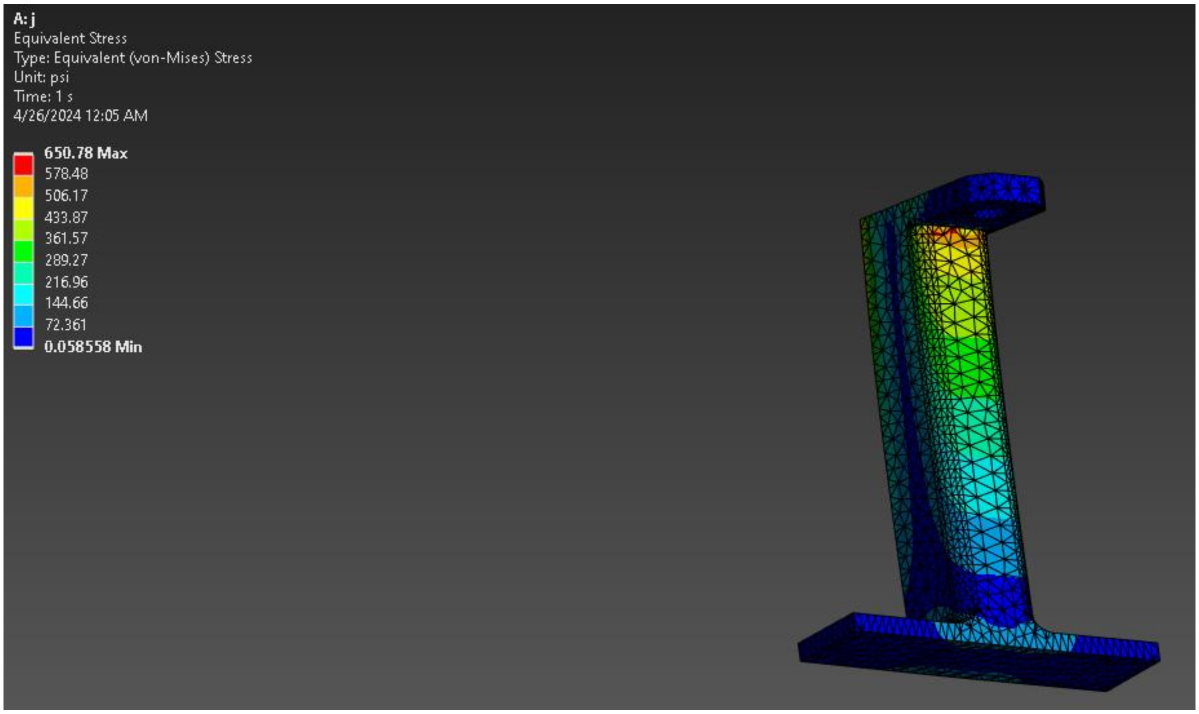

Figure 40: (Mk 3.0 FEA) - Leg, Side Force

When the side face of the battery bracket experiences a force of 1.824 lbf, a maximum stress of 704.08 psi was calculated. With an estimated yield strength of 3782.87 psi, this produced a factor of safety of 5.37. This force was created by dividing the weight of the battery by two, to account for the two battery brackets. Then, it was multiplied by an acceleration three times gravity, to give 1.824 lbf.

$$1.824\ lbf = \frac{1.216}{2}\ lb * \ 32.2\frac{ft}{s^2} * \ 3 * \frac{lbf * s^2}{32.2\ lb * ft}$$

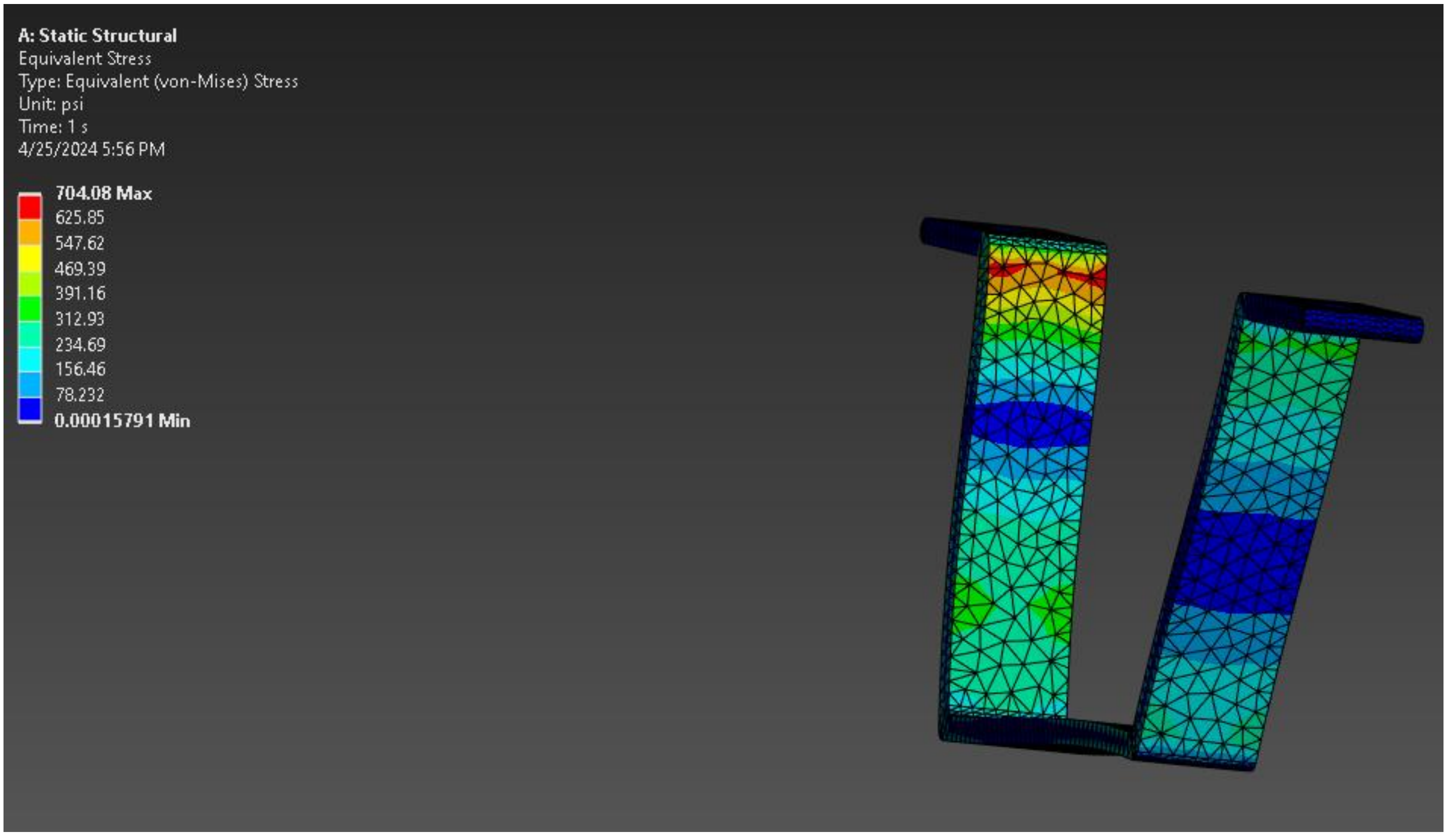

Figure 41: (MK 3.0 FEA) – Battery Bracket

Finite element analysis was not completed on the braces, as they were a temporary design feature not intended to see large loads.

7.8 Mk 3.1 Testing

All mesh sizes were 0.05 inch, along with adaptive mesh refinement with 10 max loops and refinement depth of 2. To use finite element analysis to analyze Mk 3.1, all of the same simulations as shown in previous designs were done. The drone's mass was reduced in this final redesign, so smaller forces were calculated.

For each arm, a maximum stress of 1529.9 psi was calculated from a force of 4.53 lbf. With an estimated yield strength of 3782.87 psi, this produces a factor of safety of 2.47. The total weight of this drone design, hardware, and 3 lbs of cargo was 6.040 lb.

$$4.53\,lbf = 1.51\,lb * 32.2\frac{ft}{s^2} * 3 * \frac{lbf * s^2}{32.2\,lb * ft}$$

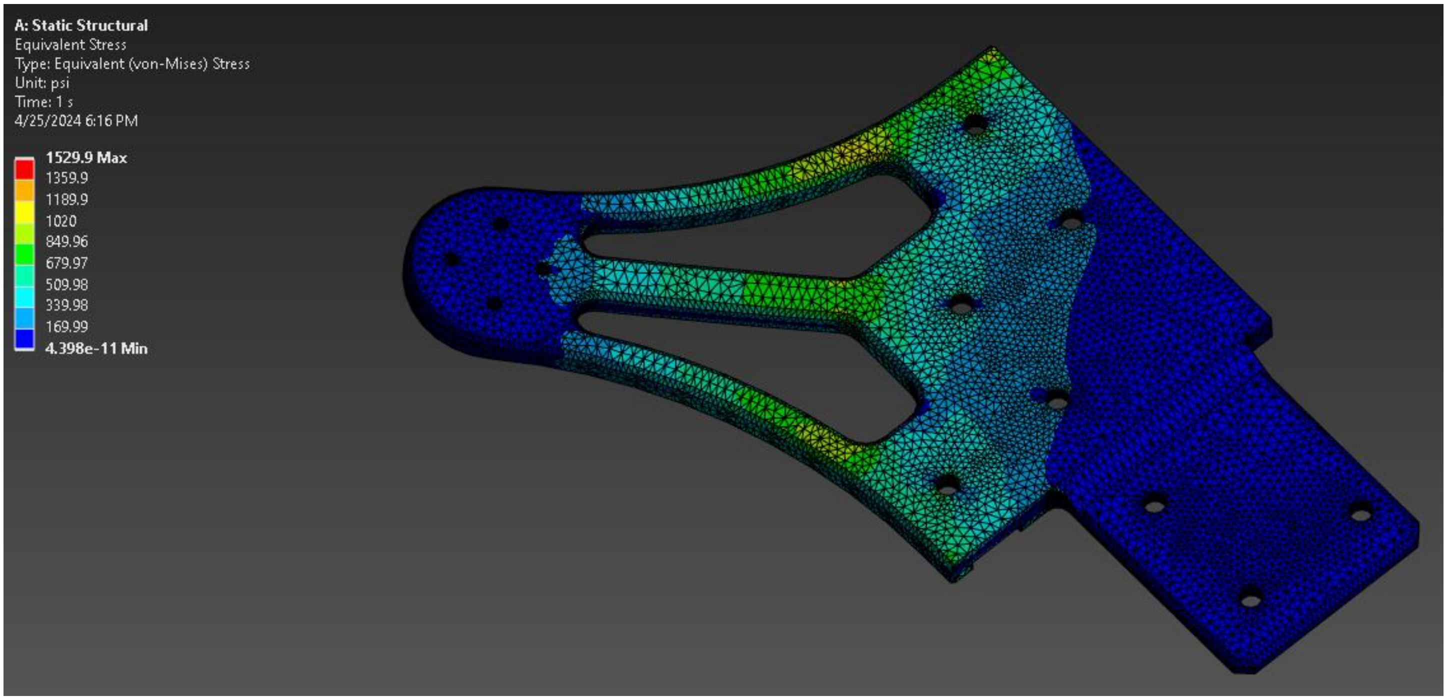

Figure 42: (Mk 3.1 FEA) – Arm

When the bottom face of the leg experiences a force of 6.04 lbf, a maximum stress of 1817.5 psi was calculated. With an estimated yield strength of 3782.87 psi, this produces a factor of safety of 2.08.

$$6.04\ lbf = 1.51\ lb * \ 32.2\frac{ft}{s^2} * \ 4 * \frac{lbf * s^2}{32.2\ lb * ft}$$

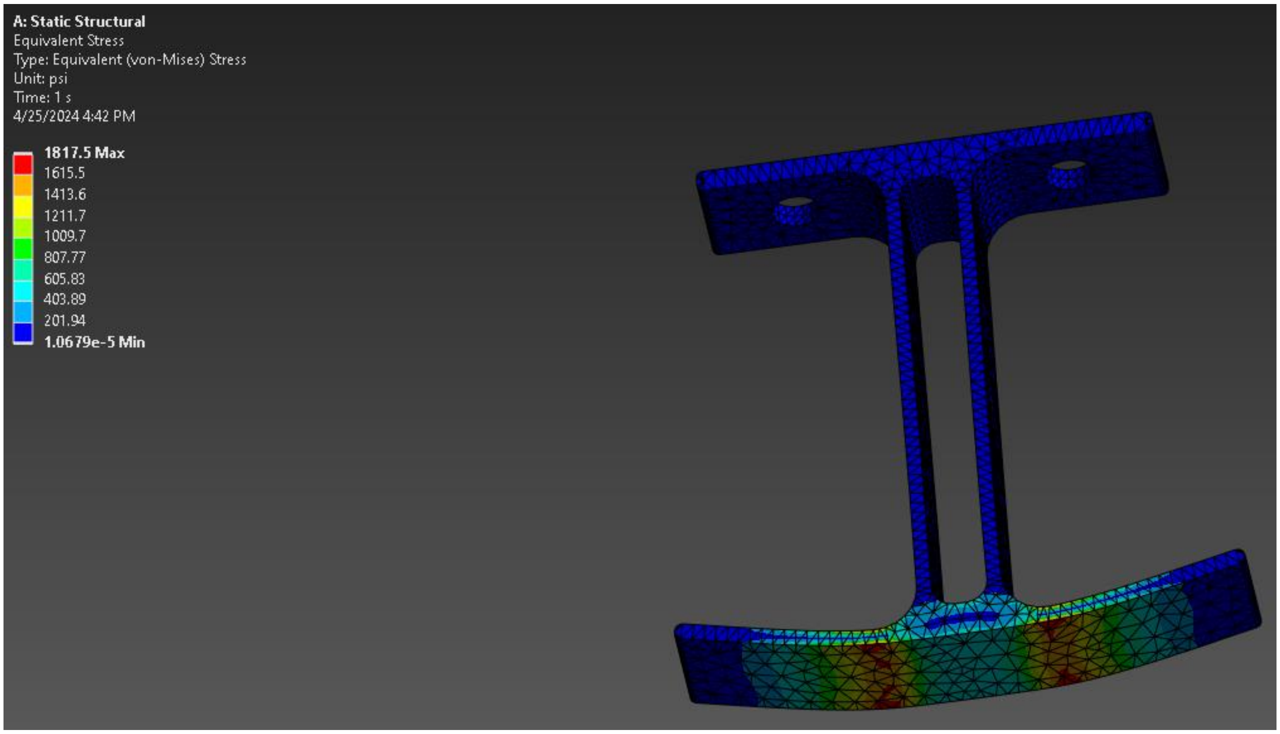

Figure 43: (Mk 3.1 FEA) – Leg, Upward Force

When the leg is impacted on the side face of the bottom part of the leg by a side force of 4.03 lbf, a maximum stress of 1822.9 psi was calculated. With an estimated yield strength of 3782.87 psi, this produces a factor of safety of 2.08.

$$4.03\ lbf = 1.51\ lb * \ 32.2\frac{ft}{s^2} * \ 2.67 * \frac{lbf * s^2}{32.2\ lb * ft}$$

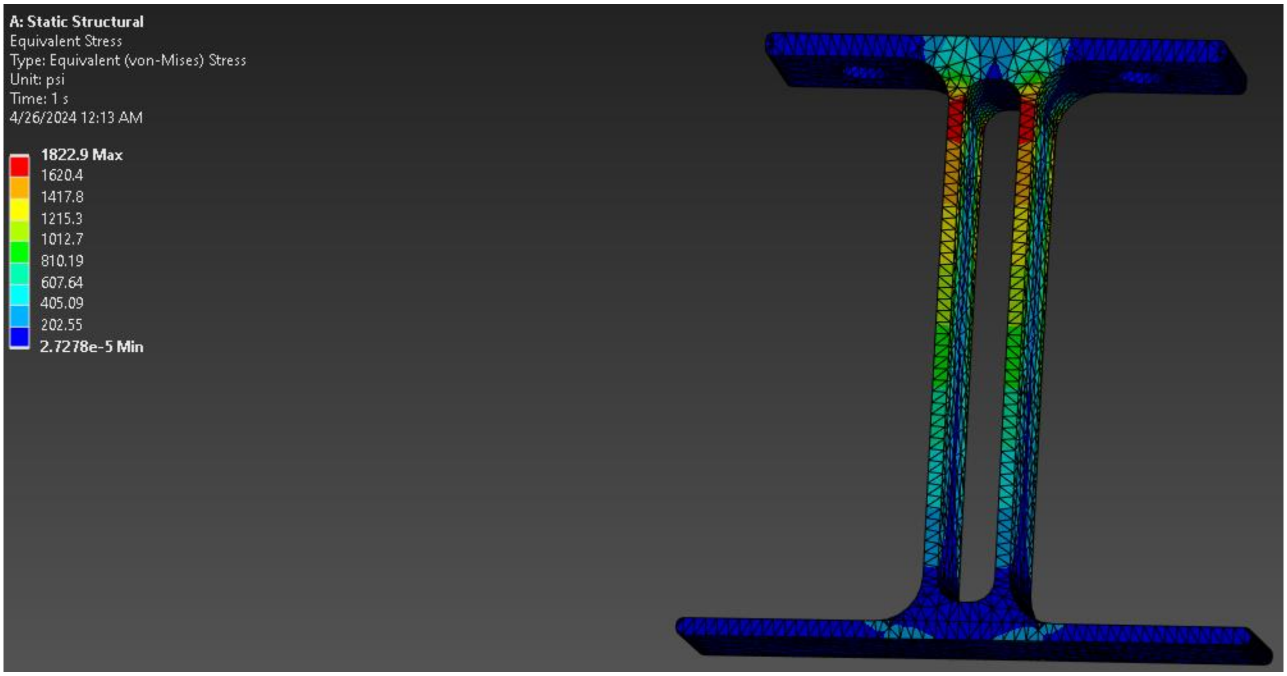

Figure 44: (Mk 3.1 FEA) - Leg, Side Force

When the side face of the battery bracket experiences a force of 1.824 lbf, a maximum stress of 2031.1 psi was calculated. With an estimated yield strength of 3782.87 psi, this produced a factor of safety of 1.86.

$$1.824\ lbf = \frac{1.216}{2}\ lb * \ 32.2\frac{ft}{s^2} * \ 3 * \frac{lbf * s^2}{32.2\ lb * ft}$$

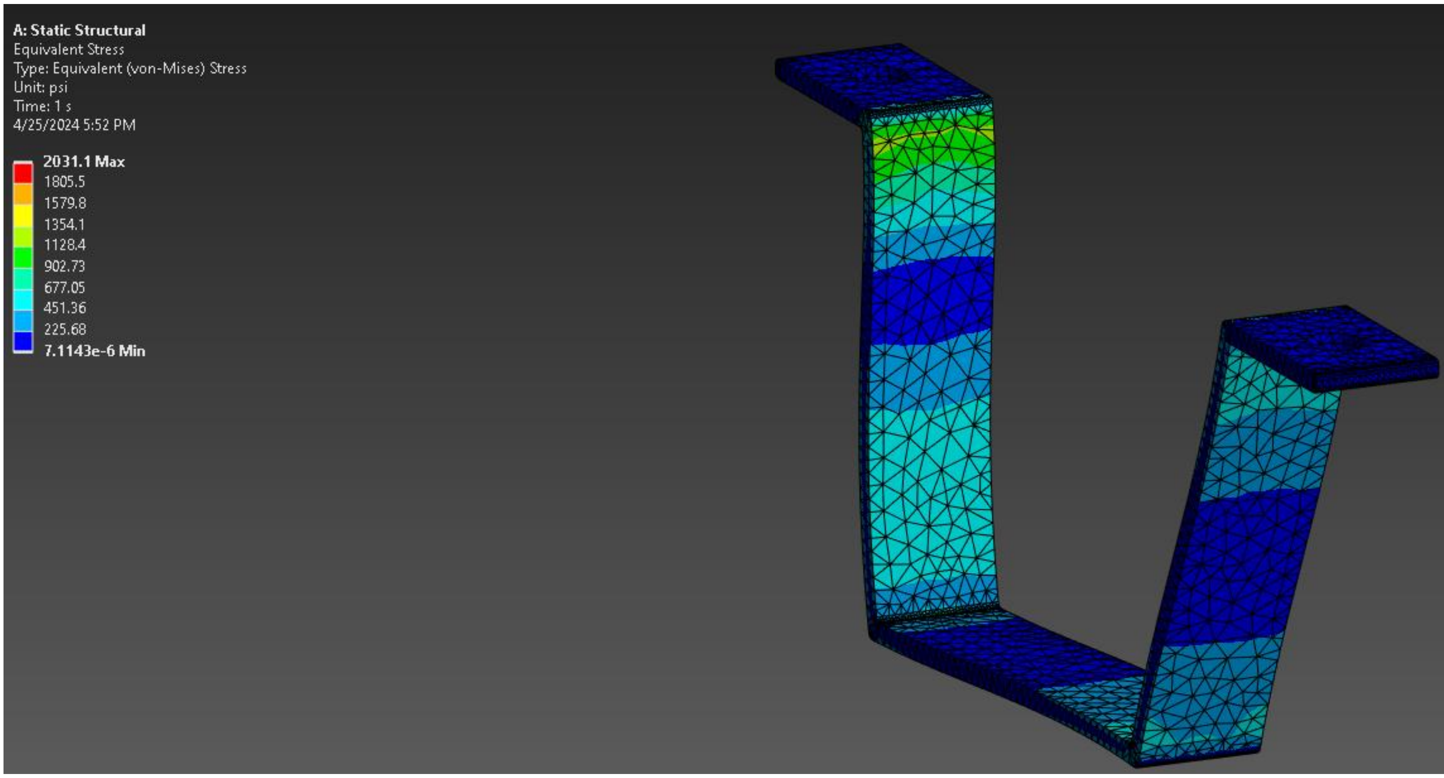

Figure 45: (Mk 3.1 FEA) – Battery Bracket

7.9 Thrust Testing (Mk 3.1)

Thrust testing was completed on the flight ready, final design of the drone by replacing two of the legs with leg brackets and the other two legs with a bracket for a force meter to hook onto. Then, the drone's leg brackets slotted through U-brackets that were screwed into wood. The wooden planks were secured in place by multiple bricks. This test setup allowed for the drone to be restricted to only moving up and down.

Figure 46: Mk 3.1 Thrust Testing

Finally, a force meter was hooked onto the force meter bracket. This restricted the drone from flying up and away, while providing accurate data on how much thrust the entire drone is producing. After repeated tests, the force meter consistently measured 5.8 lbf. The drone weighs 3.040 lbs all together. Accounting for the weight of the drone, the total thrust produced by the motors and propellors was 8.840 lbf. This was smaller than expected, as the theoretical thrust per motor was 4.4092 lb (2 kg), resulting in a total thrust of 17.627 lbf.

If the same logic is carried over from the results of our preliminary testing with the commercial drone, the drone is able to carry a payload of approximately 2.9 lbs. This number is half of the total payload capacity, since the testing drone was able to lift 2 ounces but could be flown with only 1 ounce of extra weight.

Reasons the experimental thrust was smaller than the theoretical thrust include inefficiency from the airfoil, unknown control inefficiencies, aerodynamic interactions with the body, and real-world inefficiencies from the motors. Since our lift was calculated in a relatively uncontrolled environment, the thrust produced was less than what the manufacturer produced in a static thrust test. The efficiency of the propellors used may be smaller than the efficiency of the propellors used in the experimental tests. Furthermore, necessary drone geometry on the arms of the drone may have negative aerodynamic consequences that reduce the thrust.

The experimental thrust was expected to be smaller than the theoretical thrust, but not to the degree seen. Further testing and investigation would provide more reasons for the reduced thrust, but that experimentation is outside of the scope of this project.

8. Conclusion

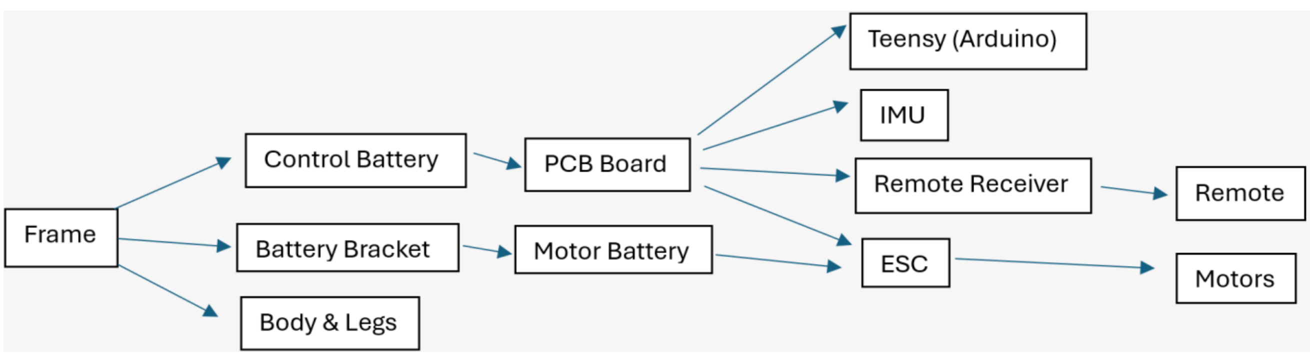

Figure 47: Drone Structure Diagram

Figure 48: Final Design (Mk 3.1)

This project has provided each member with an impactful learning experience. Despite the various hardships, the team was successful and a functional, operational, flying drone was created.

8.1 Accomplishments

The overall accomplishment for this project was creating a 3D printed drone that was not only able to fly, but could also produce enough thrust to fly with a payload attached. To accomplish the first part of the goal, we produced a fully functioning drone that was able to fly. To accomplish the second part, we were able to test the thrust capacity of our drone and verify that it is able to lift enough weight to make it a viable option for payload delivery. In addition to these two metrics, we were also able to minimize the weight of the frame through design and stress analysis, allowing us to ensure that the body will not break under normal use.

8.2 Uncertainties

It is not sure what type of long-term performance will be seen by the drone. While it is unlikely any fatigue failure will occur, if PLA material is used, the material will weaken with time if it experiences aggressive outdoor conditions constantly. If the drone is to be stored outdoors, it is recommended to use a different material like ABS.

In addition, there is little data on the batteries and motors used. While no manufactured based issues were experienced with these components, the long-term reliability of them has not been verified.

8.3 Ethical Considerations

There are countless uses for a cargo drone of this capacity. While it has been designed for certain intended purposes, it is possible it could be used for other purposes. For example, drones are often used in modern military operations. Furthermore, it is possible the drone can collide into and injure a person by accident. Until a user does proper PID tuning, the drone's stability is not ideal.

8.4 Future Work

The open-endedness of this project allows for unlimited future work to take place. The platform we have developed can be taken in countless different directions, due to the simplicity and modularity of our design. Some of the specific modifications and improvements that can be made include cargo attachments specific to the consumers intended payload, increasing overall size to increase payload capacity, PID fine tuning to optimize control, and adding in additional capabilities such as GPS, altitude lock, and cameras. Furthermore, more extensive testing can be completed on the drone, especially on the electronic aspect. No long-term testing was done to see what sort of battery life will be experienced. Also, it could be important to complete a testing scenario where the motors are subjected to full throttle for an extended period of time to ensure there are no overheating issues or other complications.

Acknowledgements

ASME. (2023). *IAM3D Innovative Additive Manufacturing 3D Challenge.* Retrieved from https://efests.asme.org/competitions/asme-innovative-additive-manufacturing-3d-challeng

Bambu Labs. (n.d.). *Bambu Filament.* Retrieved from https://store.bambulab.com/collections/bambu-lab-3d-printer-filament

Dai, S., Deng, Z. C., Yu, Y. J., Zhang, K., Wang, S. H., & Ye, J. (2020). Orthotropic elastic behaviors and yield strength of fused deposition modeling materials: Theory and experiments. *Polymer Testing, 87,* 106520. https://doi.org/10.1016/j.polymertesting.2020.106520

Draganfly. (n.d.). *Heavy Lift Drones.* Retrieved from https://draganfly.com/products/heavy-lift/

Federal Aviation Administration. (n.d.). *Do I need to register my drone and if so, how do I register?* Retrieved from https://www.faa.gov/faq/do-i-need-register-my-drone-and-if-so-how-do-i-register

Federal Aviation Administration. (n.d.). *Recreational flyers & modeler community-based organizations.* Retrieved from https://www.faa.gov/uas/recreational_flyers

Federal Aviation Administration. (2020, October 6). *Small Unmanned Aircraft Systems (UAS) Regulations (Part 107).* Retrieved from https://www.faa.gov/newsroom/small-unmanned-aircraft-systems-uas-regulations-part-107

IEEE. (2020, November 11). *Additive Manufacturing Drone Design Challenge.* Retrieved from https://ieeexplore.ieee.org/document/9249152/

Liang, O. (2023, January 28). *Understanding LiPo Batteries.* Oscar Liang. Retrieved from https://oscarliang.com/lipo-battery-guide/#Capacity

Massive Dimension. (n.d.). *Massive Dimension Materials.* Retrieved from https://massivedimension.com/collections/materials/

Rehm, N. (2020, January). *dRehmFlight VTOL Flight Controller.* Retrieved from https://github.com/nickrehm/dRehmFlight

Sounders, S. (2019, January 16). *Researchers Investigate Tensile Properties of 3D Printed PLA Specimens: Is 80% Infill Best.* Retrieved from https://3dprint.com/233916/tensile-properties-of-3d-printed-pla/#:~:text=%E2%80%9CIt%20has%20resulted%20in%20the%20ultimate%20tensile%20strength,807.489%20MPa%20and%20yield%20strength%20of%2026.082%20MPa.

Vulcan UAV. (n.d.). *Vulcan UAV Aircraft.* Retrieved from https://vulcanuav.com/aircraft/

Liang, O. (2023, January 28). *Understanding LiPo Batteries.* Oscar Liang. Retrieved from https://oscarliang.com/lipo-battery-guide/#Capacity

Appendix A - Requirement and Verification Table

The final mechanical design has been verified to operate successfully under the loads and conditions it sees through FEA and experimental flight tests. All parts reach the target 1.5x factor of safety to yield. Furthermore, all surpass 2.0 factor of safety to yield, except for the battery brackets.

	Arm	Leg, Upward Force	Leg, Side Force	Battery Bracket
MK 2.0	1.205	1.48	1.18	NA
Mk 2.1	0.5	1.94	2.8	NA
Mk 3.0	2.66	4.04	5.81	5.37
Mk 3.1	2.47	2.08	2.08	1.86

Table 8: Factor of Safety Data

Appendix B - Codes and Standards Used

According to the Federal Aviation Administration, all drones weighing more than 0.55 pounds need to be registered and have their registration number displayed on the exterior (FAA). As the designers of the drone, it is essential that this is clearly explained to any user. Furthermore, the drone will have an age limit of 16 years old per FAA regulations (FAA). Finally, to keep within restrictions, the drone's software coding will set a maximum allowable altitude of 400 feet (FAA). While a proximity sensor was outside of the scope of this project, future work includes assessing and solving this standard.

Code/Standard Name	Applications that Comply
FAA Drone Altitude	Max altitude of 400ft
FAA Drone Age Limit	User must be 16 years of age or older
FAA Drone Registration	Drones greater than 0.55 lbs must be registered.